

Review

Progress in Electrochemical Biosensing of SARS-CoV-2 Virus for COVID-19 Management

Md. Mahbubur Rahman 

Department of Applied Chemistry, Konkuk University, Chungju 27478, Korea; mahbub1982@kku.ac.kr

Abstract: Rapid and early diagnosis of lethal coronavirus disease-19 (COVID-19) caused by the severe acute respiratory syndrome coronavirus 2 (SARS-CoV-2) is an important issue considering global human health, economy, education, and other activities. The advancement of understanding of the chemistry/biochemistry and the structure of the SARS-CoV-2 virus has led to the development of low-cost, efficient, and reliable methods for COVID-19 diagnosis over “gold standard” real-time reverse transcription-polymerase chain reaction (RT-PCR) due to its several limitations. This led to the development of electrochemical sensors/biosensors for rapid, fast, and low-cost detection of the SARS-CoV-2 virus from the patient’s biological fluids by detecting the components of the virus, including structural proteins (antigens), nucleic acid, and antibodies created after COVID-19 infection. This review comprehensively summarizes the state-of-the-art research progress of electrochemical biosensors for COVID-19 diagnosis. They include the detection of spike protein, nucleocapsid protein, whole virus, nucleic acid, and antibodies. The review also outlines the structure of the SARS-CoV-2 virus, different detection methods, and design strategies of electrochemical SARS-CoV-2 biosensors by highlighting the current challenges and future perspectives.

Keywords: SARS-CoV-2; electrochemical transduction; immunosensors; aptasensors; bioreceptors; serological test



Citation: Rahman, M.M. Progress in Electrochemical Biosensing of SARS-CoV-2 Virus for COVID-19 Management. *Chemosensors* **2022**, *10*, 287. <https://doi.org/10.3390/chemosensors10070287>

Academic Editor: Danila Moscone

Received: 31 May 2022

Accepted: 16 July 2022

Published: 20 July 2022

Publisher’s Note: MDPI stays neutral with regard to jurisdictional claims in published maps and institutional affiliations.



Copyright: © 2022 by the author. Licensee MDPI, Basel, Switzerland. This article is an open access article distributed under the terms and conditions of the Creative Commons Attribution (CC BY) license (<https://creativecommons.org/licenses/by/4.0/>).

1. Introduction

Since the first case in December 2019 in Wuhan, China, the global outbreak of severe acute respiratory syndrome coronavirus 2 (SARS-CoV-2) has resulted in a life-threatening respiratory infectious coronavirus disease-19 (COVID-19) that has significantly affects the global human health, socio-economy, education, national financial policies, and other activities [1,2]. World Health Organization (WHO) declared COVID-19 as a pandemic on 12 March 2020, due to the rapid human-to-human transmission of the virus with the primary symptoms of fever, coughing, short breathing, etc. [3]. The human-to-human rapid transmission of this virus can occur through the droplet, contact, airborne, fomite, fecal-oral, and bloodborne transmissions.

A person affected with SARS-CoV-2 virus or a COVID-19 patient can remain asymptomatic without showing any signs or mild symptoms [1–3]. These asymptomatic COVID-19 patients are the major spreaders of the SARS-CoV-2 virus. Therefore, within a short time, the SARS-CoV-2 virus spread all the six continents of the world with the total number of cases as of 29 May 2022 was over 531 million and total deaths of over 6.31 million [4]. Even though about 65% of the world population has been vaccinated with at least one dose of WHO-approved vaccines [5], the number of virus-infected people and the associated deaths are still increasing. This is mainly due to the mutation of the SARS-CoV-2 virus over time by genetic variation in the population of circulating viral strains that limit the efficacy of COVID-19 vaccines [6].

Thus, the best solution to control this lethal disease is still isolation of the infected patients through the earlier detection of COVID-19. At present, real-time reverse transcription-polymerase chain reaction (RT-PCR) is the “gold standard” method for diagnosing COVID-

19 disease that is based on the molecular testing of single-strand ribonucleic acid (ssRNA) from the SARS-CoV-2 virus (Figure 1a). Nevertheless, RT-PCR testing is time-consuming, costly, and requires a specialized laboratory setup with expensive instrumentations and trained personnel [7,8]. Furthermore, the highly contagious nature SARS-CoV-2 virus could enable its faster human-to-human transmission during the sample collection and analyses.

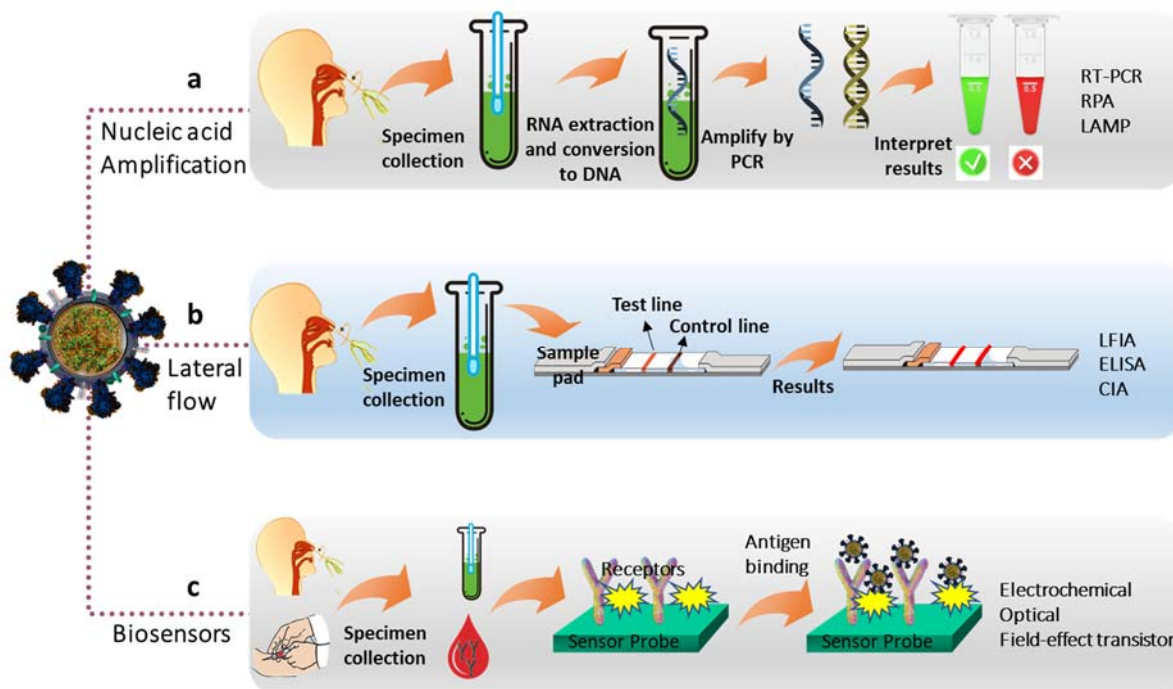


Figure 1. Schematic of the diagnosis methods of COVID-19. (a) Molecular testing based on nucleic acid amplification assays, (b) lateral flow immunoassay, and (c) biosensors.

To overcome these drawbacks, several other molecular testing based on isothermal nucleic acid (NA) amplification assays, such as loop-mediated isothermal amplification (LAMP), recombinase polymerase amplification (RPA), deoxyribonucleic acid (DNA) nano-scaffold-based hybrid chain reaction, and NA sequence-based amplification, have already been reported (Figure 1a) [9–12]. These methods also exhibit some certain limitations along with their advantages of being low cost, rapid analyses, and highly sensitive and specific. For example, LAMP and RPA methods require the design of a complex primer, and the LAMP method is unable to perform multiplex amplification [10].

In comparison to the above diagnosis methods, lateral flow immunoassay (LFIA) platforms with optical detection (colorimetry/fluorescence), enzyme-linked immunosorbent assay (ELISA), chemiluminescent immunoassay (CIA), and electrochemistry-based serological test (detection of antibody and antigen) have received much attention for diagnosis COVID-19 (Figure 1b) [13–17]. In particular, electrochemistry-based SARS-CoV-2 virus detection systems have received great potential over ‘gold standard’ RT-PCR, NA amplification assays, and optical methods.

This is due to the superior advantages of electrochemical biosensors and immunosensors, including a short reading time, require a small volume of samples, miniaturization ability, point-of-care (POC) and point-of-need (PON) testing, and high sensitivity and specificity [16–20].

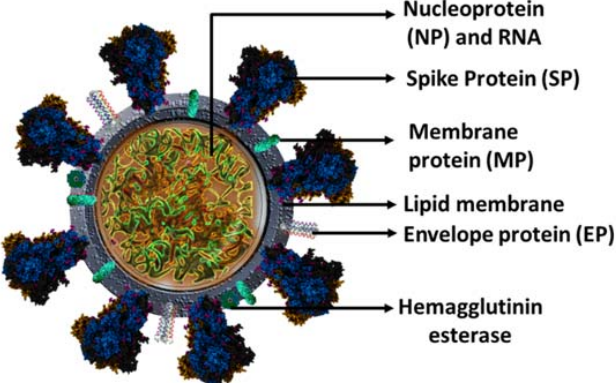
Furthermore, electrochemical biosensors and/or immuno-sensors are capable of label-free and label-based diagnosis of SARS-CoV-2 virus by exploiting redox indicators and labels [21,22]. Accordingly, a larger number of electrochemical biosensors and immunosensors have been developed for diagnosing COVID-19 by detecting antibodies, antigens (structural proteins), and nucleic acids of SARS-CoV-2 along with the development of novel

electrode modifiers and fabrication methods (Figure 1c) [9,16,17,23,24]. This review article aims at providing recent progress on electrochemical biosensors and immunosensors by reviewing about 50 research articles for the diagnosis of the SARS-CoV-2 virus along with the general mechanism of detection and chemical structure of the virus by highlighting the current challenges and future perspectives.

2. Structure of the SARS-CoV-2 Virus

The SARS-CoV-2 virus is a member of the coronavirus family with a spherical shape (diameter ~130 nm), a genome size of approximately 30 kb, and ‘spike-like structures’ all over its surface [16,25]. The genome of SARS-CoV-2 is similar to most coronaviruses, specifically, it is almost 80% and 50% similar to the SARS-CoV and middle east respiratory syndrome coronavirus (MERS-CoV), respectively [26]. SARS-CoV-2 genome encodes four structural proteins (nucleocapsid protein (NP), spike glycoprotein (SP), membrane protein (MP), and envelope protein (EP)) (Table 1), and sixteen non-structural proteins (NSPs) [26]. NSPs generally mediate RNA processing and replication/transcription, modulating the survival signaling pathway of the host cell, separating the translated protein, binding RNA, etc. [27].

Table 1. Structure of the SARS-CoV-2 virus and the mass and function of its structural proteins.



Protein	Mass (kDa)	Function
SP	~180	Binds and fuse to the host cell receptor and induces infection, and transmission.
NP	~10	Binding to the viral RNA genome critical for viral replication and genome packaging.
MP	~45–60	Viral assembly and shaping viral envelope.
EP	~ 25–30	Formation of the viral envelope.

Source: References [26–34].

Among the structural proteins, NP (mass of ~10 kDa) is an important antigen for SARS-CoV-2 that contribute to packaging viral RNA within the viral envelope and forms a ribonucleoprotein complex called nucleocapsid, in which RNA carries the virus genetic information [28,29]. Furthermore, the NP of the SARS-CoV-2 affects host cell responses and contributes to regulating the viral life cycle. The SP (mass of ~180 kDa) is a transmembrane homo-trimer with two subunits (S1 and S2) and functioning the virus adhesion and infection of a host cell [30,31]. The S1 subunit contains a receptor-binding domain (RBD) attached to a host receptor, whereas the S2 subunit enables the viral and host membrane fusion [31].

The small-sized EP of SARS-CoV-2 with a mass of ~25–30 kDa is composed of an N-terminal transmembrane domain followed by a C-terminal domain [32]. The main functions of EP are the formation of the viral envelope required to induce membrane curvature for viral assembly [33]. EP also mediates host immune responses and contributes to the virulence phases of the viral life cycle. The MP of SARS-CoV-2 is about 98% similar to the MP of SARS-CoV, while it is only 38% with the MP of MERS-CoV [34]. The key role of MP is viral assembly and shaping envelope in conjunction with EP [33].

3. Designing Electrochemical SARS-CoV-2 Virus Biosensors

3.1. Antibody Biosensors

The antibody test is principally based on the detection of antibodies developed in individuals due to exposure to the SARS-CoV-2 virus [35]. The electrochemical antibody-based

biosensors probe is based on the utilization of suitable nanomaterials (e.g., self-assembled monolayer, functionalized graphene, and conducting polymer) modified electrodes for the immobilization of SARS-CoV-2 structural proteins [36–38]. Subsequently, the SARS-CoV-2 structural proteins are used to anchor the antibodies (anti-IgG or anti-IgM), created in the biological body fluids of COVID-19 infected patients (Figure 2) [37].

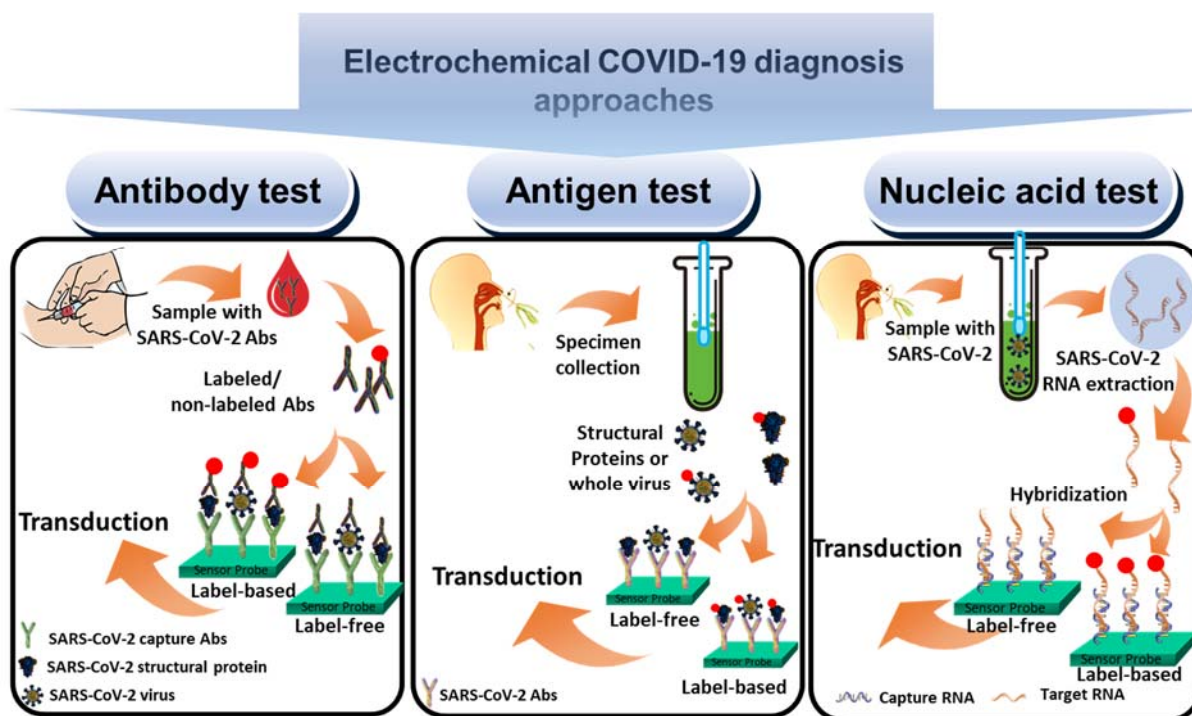


Figure 2. Schematic of the electrochemical strategies of COVID-19 diagnosis.

For a label-free detection, the anchored SARS-CoV-2 antibodies induce a variation in current, potential, and resistance of the redox indicator (e.g., $[\text{Fe}(\text{CN})_6]^{3-/4-}$, $[\text{Ru}(\text{NH}_3)_6]^{3+}$, etc.) and enabling the label-free diagnosis of COVID-19 [21,22]. In contrast, for label-based detection of SARS-CoV-2 antibodies, the representatives' antibodies can be functionalized with labels (e.g., quantum dots, redox-active molecules, and low-dimensional carbon materials) prior to the attachment with the biosensor probe [39]. Upon anchoring the labeled antibodies with a biosensor probe, the labels generate current responses suitable for the detection/determination of the SARS-CoV-2 virus with high specificity and selectivity.

Label-free sensors are preferable to label-based sensors due to their less complicated designs, short preparation time, and low cost [40]. However, lack of sensitivity, cross-reactivity, and interference are major disadvantages of label-free sensors for their practical application [39]. Even though antibody-based label-free and label-based diagnostic systems for SARS-CoV-2 and other viruses are rapid and highly specific, their clinical efficacy for SARS-CoV-2 infection testing is restricted, as it may take several days to weeks to develop a detectable antibody response in COVID-19 patients after starting to show the symptoms [35].

3.2. Antigen Biosensors

The antigen test for the diagnosis of SARS-CoV-2 infection is highly sensitive and accurate and capable of rapid detection of the virus in clinical samples [23]. Therefore, antigen tests have received emergency authorization from the food and drug administration (FDA) to diagnose SARS-CoV-2 [41]. For a simple label-free electrochemical detection of the SARS-CoV-2 virus, the protein receptor antibodies (anti-SARS-CoV-2 SP, anti-SARS-CoV-2 NP, anti-SARS-CoV-2 EP, and anti-SARS-CoV-2 MP) can be immobilized onto

nanomaterial-modified electrodes. Subsequently, the whole SARS-CoV-2 virus or the corresponding structural proteins can bind with the sensors probe (Figure 2) [23,40].

This induces discrimination of the current, potential, and resistance signals of the redox indicators, enable the label-free diagnosis of COVID-19 [21,22]. Aaptamers, molecularly imprinted polymer (MIP), and angiotensin-converting enzyme 2 (ACE2) can also be used as receptors for the construction of antigen biosensors. In contrast, for label-based detection of the SARS-CoV-2 virus and the corresponding structural proteins, prior labeling of them is required before anchoring to the sensor probe. Upon anchoring the labeled-virus or labeled-structural proteins attached to the biosensor probe can generate a current response suitable for the detection/determination of the virus with high specificity and selectivity [39,40].

3.3. Nucleic Acid Biosensors

Single-strand capture or probe NA (ss-NA) can bind with the target complementary NA (c-NA) that forms the basis of gene chips, DNA computers, and NA biosensors [22,42,43]. The hybridization between the probe ss-NA and target c-NA converts the recognition event into a measurable electrical signal. Based on this basis, electrochemical biosensors can be developed to identify NA copies selectively in SARS-CoV-2 for diagnosing COVID-19 infection (Figure 2). Similar to the antibody and antigen test, both label-free and label-based electrochemical NA biosensors can also be developed. For this purpose, a sensor probe can be developed by immobilizing labeled or label-free probe NA onto a nanomaterial-modified electrode.

In a label-free electrochemical SARS-CoV-2 NA biosensor, the virus c-NA genomic sequence can bind with the sensor surface by the hybridization with the probe-NA and induces a variation in electrochemical signals of a redox mediator to diagnose COVID-19. While, for a label-based system, the label/molecular tag onto the probe NA or target c-NA can generate a current response upon hybridization between capture NA and target c-NA, suitable for the detection of SARS-CoV-2 virus with high sensitivity and selectivity. However, the large genomic sequence of the SARS-CoV-2 virus (~30 kb) can easily form complicated secondary structures, thus, limiting the accessibility of probe NA to the target c-NA [44]. Furthermore, the low viral load in real-world samples can induce a low sensitive signal in a NA biosensor for an unamplified SARS-CoV-2 gene in a COVID-19 patient [44].

4. Electrochemical Biosensors for the Detection of SARS-CoV-2 Virus

4.1. Electrochemical Antibody-Based Detection of SARS-CoV-2 Virus

Antibodies, such as anti-IgG, anti-IgM, and immunoglobulin A (anti-IgA), can be developed from the COVID-19 patients' body fluids that can be used to detect SARS-CoV-2. The recent immuno-chromatographic study suggests that both IgG and IgM antibodies exhibit 11.1%, 92.9%, and 96.8% sensitivity of SARS-CoV-2 detection at the early stage (several days to weeks after the COVID-19 infection), intermediate stage (1–2 weeks after the onset), and late-stage (more than 2 weeks), respectively [45,46].

Anti-IgA is another major antibody in the respiratory tract that is produced by B-lymphocytes and expressed after 2 weeks of COVID-19 infection [45,46]. Thus, the detection of antibodies in human blood serum samples by developing highly sensitive electrochemical biosensors can be an effective tool for diagnosing COVID-19 infection at the early stage of infection, in which SP and NP can serve as antigens for the specific binding of antibodies.

The IgG antibody is a lighter and smaller (~150 kDa) antibody compared to the IgM antibody (~900 kDa) with two antigen-binding sites [47,48]. The anti-IgG can be detected only after a week of infection without altering its concentration for a long period after infection and after several weeks, anti-IgG reactivity reaches >98% [49]. Thus, the detection of anti-IgG has attracted considerable attention over IgM and IgA antibodies. Some selected examples for the detection of anti-IgG are outlined below.

Electrode materials play a crucial role in improving the sensitivity of electrochemical detection. This is because electrode materials with high surface area and functionality could increase the amount of immobilized target-specific antigens or antibodies [50,51]

and induce to enhance the detection sensitivity with a wide dynamic range and low limit of detection (LOD). The high electrical conductivity is also crucial for obtaining high sensitivity, which can be achieved by providing an efficient electron transport channel for the redox reaction of a redox probe or target analyte.

Among the various nanomaterials for the modification of electrode surfaces for biosensor development, graphene, and its related materials, including graphene oxide (GO) and reduced graphene oxide (rGO), have attracted significant interest [52,53]. This is mainly due to their high chemical functionality and surface area, solution processability, and excellent electron transporting capability [52]. Accordingly, Yakoh et al. reported a label-free electrochemical immunosensor based on a GO-modified paper electrode that can successfully detect IgG antibodies (Figure 3a) [54].

The IgG antibody can specifically bind with the SARS-CoV-2 SP antigen-modified GO/paper immunosensor probe that induces the high specificity and sensitivity of COVID-19 diagnosis in clinical serum samples. Upon forming the anti-IgG/SP antigen complex, the redox activity of $[\text{Fe}(\text{CN})_6]^{3-/4-}$ is decreased with increasing the concentration of IgG antibodies. This can be ascribed to the insulating nature of antibodies, which induce a decrease in the redox peak current by increasing the charge transfer resistance (R_{ct}) as the electrode/electrolyte interface.

Concurrently, the immunosensor exhibits a wide linear range for the detection of anti-IgG with the LOD of 1 ng/mL. In another report, Ali et al. prepared an ultrasensitive and label-free 3D biosensor based on a micropillar array of Au nanoparticles (AuNPs) coated with rGO sheets (Figure 3b) [55]. Subsequently, the SARS-CoV-2 NP was immobilized onto the AuNPs/rGO-modified micropillar array via (3-dimethylaminopropyl)-N'-ethylcarbodiimide (EDC)-N-hydroxysulfosuccinimide (NHS) coupling chemistry. Finally, the immunosensor array was integrated into a microfluidic channel to complete the electrochemical cell.

The as-prepared immunosensor could selectively bind IgG antibodies, which induces to increase in the R_{ct} for $[\text{Fe}(\text{CN})_6]^{3-/4-}$ redox couple with increasing the concentration of IgG antibodies in the detection range of 100 fM to 1 nM and the LOD of 13 fM. The same research group utilized a similar rGO-modified Au micropillar array for the immobilization of SARS-CoV-2 SP antigen via EDC-NHS coupling (Figure 3c) [56].

This label-free electrochemical microfluidic immunosensors probe could selectively bind the IgG antibodies which induces to increase in the R_{ct} values for the redox reaction of $[\text{Fe}(\text{CN})_6]^{3-/4-}$ with increasing the concentration of anti-IgG. The corresponding LOD of the immunosensor was 2.8×10^{-15} M for the detection of anti-IgG. A similar sensing electrode based on GO and Au nanostar-modified carbon-based screen-printed electrode (SPE) was developed by Hashemi et al. for the label-free detection of IgG antibodies specific for SARS-CoV-2 SP antigen with a low LOD and high sensitivity (Figure 3d) [57].

Other than GO and rGO, metal-oxide, conducting polymers, and molecular functionalization of electrodes can be effective substrates for the development of COVID-19 antibody sensors [58–61]. Li et al. prepared a label-free COVID-19 IgG antibody sensing platform based on microfluidic paper-based analytical devices (μ PADs) (Figure 3e) [58]. The carbon-coated μ PAD was modified with ZnO nanowires (NWs) using the hydrothermal method. Then, the glutaraldehyde and (3-aminopropyl)-trimethoxysilane-modified ZnO NWs electrode surface was functionalized with SARS-CoV-2 SP for the selective binding of anti-IgG, specific for COVID-19 infection. The as-prepared electrochemical impedance spectroscopy (EIS) based label-free immunosensor platform could detect IgG antibodies in human serum samples up to 1 $\mu\text{g}/\text{mL}$.

To date, electrochemical label-based detection of COVID-19 antibody is less developed compared to the label-free approaches. This is possibly due to the complicated labeling steps, long preparation time, and high cost even though label-based detection exhibited high specificity and selectivity. Ameku et al. reported a label-based method for the detection of SARS-CoV-2 specific anti-IgG based on a polyglutaraldehyde SPE (Figure 3f) [59].

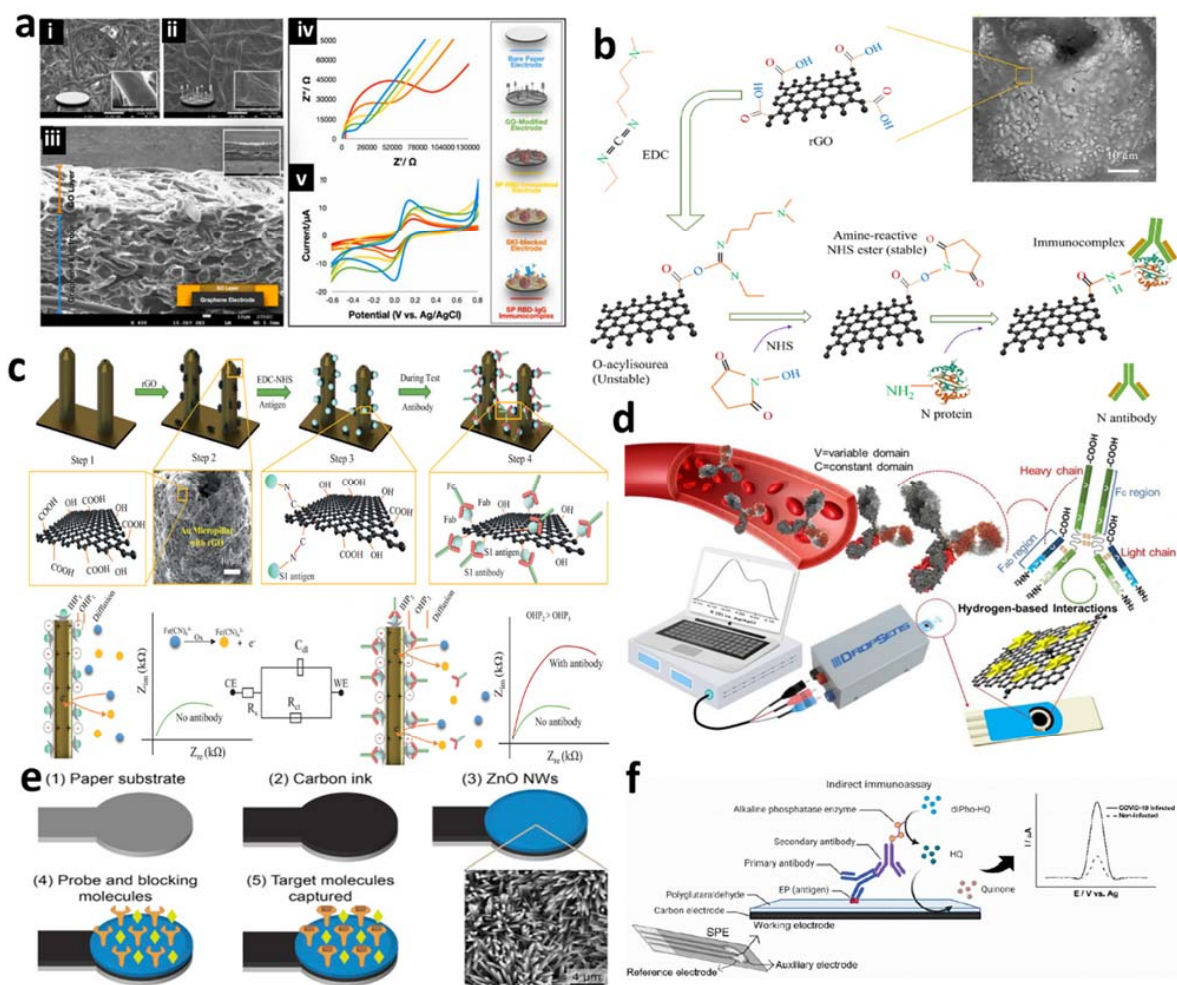


Figure 3. (a) Surface morphological FE-SEM images of the (i) bare paper and (ii) graphene oxide (GO)-modified paper with a cross-sectional image of (iii) GO/paper, corresponding to the (iv) CV and (v) EIS responses with the schematic of each modification steps for the detection of IgG antibodies (adapted with permission from ref. [54]). Copyright 2021 Elsevier. (b) Schematic of stepwise fabrication of reduced GO (rGO)-Au micropillars for IgG antibody detection (reprinted with permission from ref. [55]). Copyright 2022 Wiley. (c) Functionalization of nano-printed rGO-coated 3D Electrodes for the binding of IgG antibodies against spike protein of SARS-CoV-2, sensing principle, and interfacial properties of electrode/electrolyte interface with corresponding EIS spectrum (reprinted with permission from ref. [56]). Copyright 2021 Wiley. (d) Schematic illustration of the interaction of graphene-Au nanostar complex with IgG antibodies against the spike protein of SARS-CoV-2 (adapted with permission from ref. [57]). Copyright 2021 Elsevier. (e) Schematic of the fabrication of ZnO nanowires-modified paper electrode for EIS-based IgG antibody sensing (adapted with permission from ref. [58]). Copyright 2021 Elsevier. (f) Schematic representation of the fabrication of polyglutaraldehyde-modified SPE for the label-based detection of IgG antibody along with the electrochemical responses (adapted with permission from ref. [59]). Copyright 2022 MDPI.

The SPE electrode was functionalized with a B-cell epitope (EP) specific to the SARS-CoV-2 SP. After the binding of EP, the anti-SARS-CoV-2 IgG antibody (primary antibody) obtained from COVID-19 patient serum samples was anchored onto the sensor surface. Subsequently, a secondary antibody labeled with alkaline phosphatase (AP) was attached to the primary antibody. This AP label induces the electrocatalytic oxidation of hydroquinone (HQ) diphosphate to HQ, and the corresponding oxidation current is proportional to the concentration of IgG antibodies. This label-based platform was found to diagnose COVID-19 infection with 93% selectivity and 100% specificity.

Along with IgG antibodies, the detection of anti-IgM is also significantly important for the early diagnosis of COVID-19 infection (between 4 and 10 days). To the best of the author's knowledge, no reports are available for the electrochemical detection of IgM antibodies only for diagnosing COVID-19 infection. However, reports are available for detecting both IgG and IgM antibodies. Torrente-Rodríguez et al. developed a SARS-CoV-2 portable rapidPlex for the ultrasensitive detection of SARS-CoV-2 NP, anti-IgG, anti-IgM, and inflammatory biomarker C-reactive protein (CRP) (Figure 4a) [62].



Figure 4. (a) Schematic illustration of the RapidPlex multisensor platform wirelessly transmitted to a mobile user interface for detection of IgG and IgM antibodies of SARS-CoV-2 viral proteins and inflammatory biomarker C-reactive protein (CRP), the photograph of mass-producible sensor arrays, single disposable and flexible graphene array, and the image of the RapidPlex system attached to a printed circuit board (adapted with permission from ref. [62]). Copyright 2020 Elsevier. (b) Schematic illustration of the (i) design of portable and rapid electrochemical detection of IgG and IgM antibodies against SARS-CoV-2 spike glycoprotein, (ii) surface functionalization of the carbon-based working electrode with biotinylated receptor-binding domain protein, (iii) binding of IgG or IgM antibodies on the sensor probe and subsequent labeling with alkaline phosphatase-conjugated detection antibody, and (iv) reaction mechanism for the electrochemical oxidation of p-aminophenyl phosphate substrate (adapted with permission from ref. [63]). Copyright 2022 Elsevier.

This ultra-rapid detection platform was developed using a laser engraved 1-pyrenebutyric acid (PBA) functionalized graphene electrodes. This multiplexed sensor, specifically, for the detection of IgG and IgM antibodies was modified with SARS-CoV-2 SP for their specific binding of them via EDC and NHS chemistry. Upon anchoring the IgG and IgM antibodies onto the corresponding immunosensor probe, the electrochemical redox activity of $K_4[Fe(CN)_6]/K_3[Fe(CN)_6]$ was varied with the concentration of IgG and IgM.

This induces the ultrasensitive, highly selective, and rapid electrochemical detection of antibodies in human blood and saliva samples, which can be monitored remotely. In another report, Peng et al. prepared a portable and label-based detection platform for the detection of IgG and IgM antibodies specific for SARS-CoV-2 SP in human serum samples (Figure 4b) [63]. This sensing platform is based on a screen-printed electrode, which sequentially underwent a series of surface functionalization steps including (i) electrochemical activation, (ii) immobilization of streptavidin, (iii) hybridization of biotinylated SARS-CoV-2 SP RBD.

Then, the target primary IgG/IgM antibodies specific for SARS-CoV-2 SP, in the human serum sample, was anchored with the SARS-CoV-2 SP RBD. Subsequently, an AP labelled secondary anti-human antibody specific to IgG/IgM antibodies was bound with the IgG/IgM antibodies. This AP labeled secondary antibody catalyzes the redox reaction of p-aminophenyl during chronoamperometry (CA) with the production of the current signal.

This variation of the corresponding current responses with the variation of the concentration of IgG/IgM antibodies enables the detection of them in the range of 10.1 ng/mL–60 µg/mL and 1.64 ng/mL–50 µg/mL, respectively, with an assay time of 13 min. Some other researchers developed IgG/IgM sensing platforms based on DNA-assisted nanopore, SARS-CoV-2 SP-modified Ni(OH)₂ NPs bio-conjugate, and SARS-CoV-2 SP/GO-modified paper electrode [54,64,65]. The corresponding analytical performance of these biosensors are summarized in Table 2.

Table 2. Analytical performance of recently developed electrochemical biosensors for the detection of SARS-CoV-2 antibodies.

Electrode	Detection Method	Target Antibodies	LOD	Linear Range	Ref.
Paper-based ePAD	SWV	IgG/IgM	0.96/0.14 ng/mL	1–1000 ng/mL	[54]
AuNPs/rGO	EIS	IgG	13 fm	100 fm–1 nM	[55]
Au micropillar/rGO	EIS	IgG	2.8 fm	-	[56]
Paper-based µPADs	EIS	IgG	0.4 pg/mL	10–1000 ng/mL	[58]
Au electrode	EIS	IgG	1.99 nM	30 nM–150 nM	[60]
Au based well plate	EIS	IgG	-	-	[61]
SPE	CA	IgG/IgM	10.1/1.64 ng/mL	10.1 ng/mL–60 µg/mL and 1.64 ng/mL–50 µg/mL	[63]
Ni(OH) ₂ /SPE	DPV	IgG/IgM	0.3 fg/mL	1 fg/mL–1 µg/mL	[65]

Note: SWV = square wave voltammetry, DPV = differential pulse voltammetry.

4.2. Electrochemical Antigen-Based Detection of SARS-CoV-2 Virus

The detection of the SARS-CoV-2 virus protein antigens, including SP, NP, and whole virus, providing the possibility of early diagnosis of COVID-19. Accordingly, various strategies have recently been developed, and many of them are now commercially available for the early diagnosis of COVID-19 [66]. This section of the review discusses the recently developed antigen-based electrochemical sensors/biosensors for COVID-19 diagnosis by dividing into three subsections, namely the detection of SP, detection of NP, and detection of whole virus or virus particles.

4.2.1. Detection of Spike Proteins

The SP is the key *trans*-membrane protein of the SARS-CoV-2 virus with diverse amino acid sequences providing the precise diagnosis of COVID-19 infection [67,68]. Therefore, intensive efforts have been made for the development of electrochemical SP sensors by developing novel chemistry, electrode materials, and capture probe (e.g., antibody, aptamer, and angiotensin-converting enzyme).

Antibody capture probe-based electrochemical biosensors or immunosensors display high specificity and reliability for the detection of target biomolecules [43]. Accordingly, anti-SARS-CoV-2 capture probe-based immunosensors have received potential interest for screening SARS-CoV-2 protein antigens. Adeel et al. developed an ultrasensitive and label-free electrochemical SP sensing platform based on a functionalized self-supported graphitic carbon foil electrode (Figure 5a) [69].

The electrode was prepared by mild acidic treatment with partial oxidation and exfoliation of graphitic carbon foil electrode. The subsequent ethylenediamine functionalization of the electrode provided a suitable platform for the covalent attachment of the anti-SARS-CoV-2 SP capture probe. Upon the binding of specific SARS-CoV-2 SP onto the sensor probe, the electrochemical redox activity of the $[\text{Fe}(\text{CN})_6]^{3-/4-}$ redox couple was varied with the concentration of SP.

This enabled the detection of SP within the concentration range from 0.2–100 ng/mL with a LOD (27 pg/mL) in diluted blood plasma. A similar antibody-capture probe-based field-effect transistor (FET) was developed by Seo et al. to detect SARS-CoV-2 SP in COVID-19 infected patients' samples [70]. This graphene-based FET device was coated with anti-SARS-CoV-2 SP against the SARS-CoV-2 SP using the 1-pyrenebutyric acid N-hydroxysuccinimide ester.

The effectiveness of the FET device for binding SARS-CoV-2 SP and SARS-CoV-2 was tested using a cultivated virus, viral antigen, and nasopharyngeal swab samples. The biosensor could detect SARS-CoV-2 SP at a concentration of 100 fg/mL clinical transport medium. Similar antibody capture probe-based SARS-CoV-2 SP detection platform was developed by Malla et al. [71]. This label-based and POC biosensor is prepared using an SPE electrode modified with antibody-peroxidase-loaded magnetic beads (MBs) that could detect SARS-CoV-2 SP in the range from 3.12–200 ng/mL with the LOD of 0.20, 0.31, and 0.54 ng/mL in human saliva, urine, and serum, respectively.

Even if antibody capture probes exhibit high specificity, several limitations of antibodies, such as low stability, high cost, short shelf-life, and immunogenicity prompted to use of alternative capture probes for the development of biosensors and other biological applications [43,51]. The aptamer is one of the suitable alternatives to antibodies that can overcome the intrinsic limitations of immunosensors. Aptamers are peptide or NA (DNA or RNA) molecules with high stability, specificity, long-shelf-life, low immunogenicity, and easy synthesis and functionalization [52].

Thus, aptamers have attracted wide interest in developing electrochemical biosensors to detect various target biomolecules [43,51,52]. Idili et al. prepared a label-based electrochemical aptasensor for the detection of SARS-CoV-2 SP that is based on an Au electrode modified with methylene blue derivative (MB2) labeled aptamer (Figure 5b) [72]. The binding event of SARS-CoV-2 SP with the aptamer induces the variation of aptamer conformation, which in turn varies the position of the redox label MB2. This generated a quantitative electrochemical signal related to the variation of the concentration of SARS-CoV-2 SP.

The aptasensor could detect the picomolar level of SP with high specificity. In another report, Curti et al. reported another label-based aptasensor based on single-walled carbon nanotube screen-printed electrodes (SWCNT-SPEs) functionalized with a redox-tagged DNA aptamer [73]. The selective binding of SARS-CoV-2 SP folded the DNA aptamer which reduces the efficiency of the electron transfer between the AttoMB2 redox label and the electrode surface. Thus, the redox signal of the redox tag is suppressed by increasing

the concentration of SARS-CoV-2 SP and forms the basis of SP quantification. The aptasensor exhibited high selectivity and specificity with the LOD of 7 nM.

ACE2 is another potential and selective receptor for binding SARS-CoV-2 SP with nanomolar range affinity [74]. Furthermore, the active site of the ACE2 is located away from the SARS-CoV-2 binding site, thus, resulting in an effect on the electrochemical signal upon binding with SARS-CoV-2. Inspired by this advantage of ACE2, Vezza et al. developed an accurate and rapid diagnostic device for the detection of SARS-CoV-2 SP that is based on a printed circuit board (PCB) electrode (Figure 5c) [75].

For the fabrication of the sensing platform, the PCB electrode was modified with 1H,1H,2H,2H-perfluorodecanethiol (PFDT) followed by the ACE2 functionalization via physisorption. The selective binding of SARS-CoV-2 SP onto the sensor probe induces to decrease in the redox activity of $[\text{Fe}(\text{CN})_6]^{3-/4-}$ and increases the R_{ct} in EIS measurement by increasing the concentration of SP. This enabled the detection of SARS-CoV-2 SP with the LOD of 1.68 ng/mL. Similarly, another SP sensing platform was developed that is based on MBs and AuNPs conjugated to ACE2 for the capturing and detection of SARS-CoV-2 SP [76].

This magneto-assay modified SPE exhibited 93.7% specificity for SARS-CoV-2 SP with the LOD of 0.35 ag/mL. In another report, Lima et al. prepared a low-cost advanced diagnostic device based on AuNP-modified graphite leads. The cysteamine modification of AuNPs enabled the covalent immobilization of ACE2. The subsequent binding of SARS-CoV-2 SP to the ACE2 receptor induces a decrease in the electron transfer kinetics of $[\text{Fe}(\text{CN})_6]^{3-/4-}$ redox probe and decreases the oxidation current by increasing the concentration of SP. This label-free approach is capable of detecting SP in clinical saliva and nasopharyngeal/oropharyngeal with excellent sensitivity, specificity, and accuracy. This research further demonstrated that ACE2 is an effective, specific, and selective receptor for anchoring SARS-CoV-2 SP.

In the quest of replacing the labile and expensive biological receptor, recently, synthetic receptor or plastic antibodies, such as molecularly imprinted polymer (MIP) have received potential interest for biosensors, bioanalyses, drug delivery, and disease diagnosis [77]. In particular, MIP has attracted significant interest as a receptor for biosensors development, mainly due to its antibody-like ability to bind and discriminate between molecules, excellent chemical and thermal stability, and low cost [78]. Taking the advantages of MIPs, Ayankojo et al. developed an electrochemical biosensor for the detection of SARS-CoV-2 SP that is based on disposable Au-based thin-film electrodes (Au-TFME) chip modified with MIP film (Figure 5d) [79].

The selectivity of the MIP towards SARS-CoV-2 SP was achieved by harnessing the covalent imprinting approach between 1,2-diols moieties of SARS-CoV-2 SP and boronic acid groups of 3-aminophenyl boronic acid (APBA). The operation principle of the sensor is based on the variation of the charge transfer between the Au-TFME and $[\text{Fe}(\text{CN})_6]^{3-/4-}$ redox probe, through the imprinted pathways generated within SARS-CoV-2 SP-MIP film.

Upon the rebinding of the SARS-CoV-2 SP presence in the analyte solution, the charge transfer kinetics of the redox probe is hindered, leading to a decrease in the peak current proportional to the concentration of the SARS-CoV-2 SP. Accordingly, the sensor could detect SP within 15 min with a LOD of 64 fM in COVID-19 patient's nasopharyngeal samples. Other works related to the use of antibodies, aptamers, ACE2, and MIPs as receptors for electrochemical detection of SARS-CoV-2 SP [80–86] and their analytical performances are summarized in Table 3.

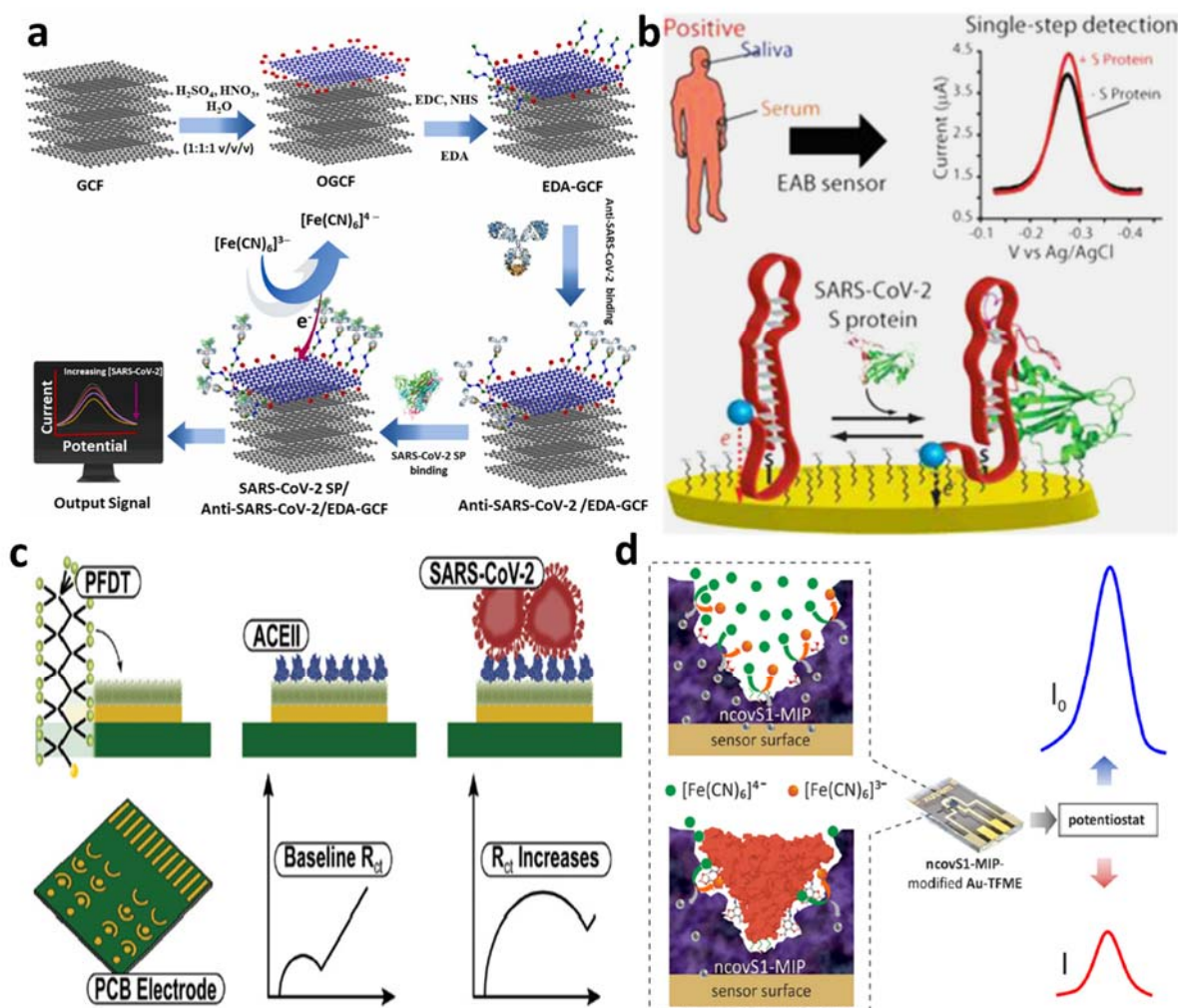


Figure 5. (a) Schematic illustration of the fabrication of self-supported ethylenediamine (EDA) functionalized graphitic carbon foil-based biosensor for detecting SP (adapted with permission from ref. [69]). Copyright 2022 Elsevier. (b) Schematic of an Au-electrode-based labeled aptasensors and the corresponding electrochemical signals for the detection of SP (adapted with permission from ref. [72]). Copyright 2022 American Chemical Society. (c) Schematic of the stepwise modification of printed circuit board with 1H,1H,2H,2H-perfluorodecanethiol (PFDT) and ACE2 receptor for the binding of SARS-CoV-2 SP along with the resultant impedance signals (adapted with permission from ref. [75]). Copyright 2021 Royal Society of Chemistry. (d) Schematic of the operation principle of SP sensing based on molecularly imprinted polymer (MIP) (adapted with permission from ref. [79]). Copyright 2022 Elsevier.

Table 3. Analytical performance of recently developed electrochemical biosensors for detecting SARS-CoV-2 SP.

Materials/Electrode	Detection Method	Receptors	Detection Medium	LOD	Linear Range	Ref.
Functionalized graphitic carbon foil	DPV	antibody	blood plasma	27 pg/mL	0.2–100 ng/mL	[69]
Graphene	FET	antibody	nasopharyngeal samples	100 fg/mL	-	[70]

Table 3. Cont.

Materials/Electrode	Detection Method	Receptors	Detection Medium	LOD	Linear Range	Ref.
MB/APBA/Antibody-HRP/GLU/SPE	SWV	antibody	human saliva	0.20 ng/mL	3.12–200 ng/mL	[71]
Au	SWV	aptamer	serum and artificial saliva	-	-	[72]
SWCNT-SPE	DPV	aptamer	PBS	7 nM	20–100 nM	[73]
PFDT/PCB	EIS	ACE2	human saliva	38.6 copies/mL	-	[75]
MB/AuNPs/SPE	DPV	ACE2	PBS	0.35 ag/mL	0.0009–360 fg/mL	[76]
Au-TFME	SWV	MIP	nasopharyngeal samples	64 fM	0–400 fM	[79]
CMCt/Au IDE	EIS	antibody	PBS	0.179 fg/mL	10^{-20} – 10^{-14} g/mL	[80]
Au	EIS	antibody	PBS	2.78 nM	30–150 nM	[81]
Cu ₂ O NCs/SPCE	EIS	antibody	PBS	0.04 fg/mL	0.25 fg/mL–1 µg/mL	[82]
Thin-film Au electrodes	EIS	aptamer	nasopharyngeal samples	-	-	[83]
AuNPs/SPCE	EIS	aptamer	PBS	1.30 pM (66 pg/mL)	10 pM–25 nM	[84]
CNF/AuNP/SPE	EIS	aptamer	PBS	7.0 pM	0.01–64.0 nM	[85]
MIP-poly(pyrrole)/Pt	Amperometry	MIP	PBS	-	0–25 µg/mL	[86]

Note: GLU = glucose, HRP = horseradish peroxidase, antibody, TFME = thin-film metal electrodes, CMCt = carboxymethylchitosan, IDE = interdigitated electrode, and NCs = nanocubes.

4.2.2. Detection of Nucleocapsid Protein

The NP of SARS-CoV-2 is a potential antigen biomarker for diagnosing COVID-19 infection since it can be available in the nasal swab, serum, and gargle solution samples of individuals after the first two weeks of COVID-19 infection [87,88].

Therefore, attempts were made to develop highly sensitive electrochemical biosensing systems based on an antibody, aptamer, and MIP receptors for detecting SARS-CoV-2 NP. Samper et al. developed a highly sensitive and label-based electrochemical immunoassay for quantitative detection of SARS-CoV-2 NP using stencil-printed carbon electrodes (SPCEs) (Figure 6a) [89]. The abundant carboxyl groups (-COOH) on the SPCEs enabled the immobilization of anti-SARS-CoV-2 NP via EDC/NHS coupling. Subsequently, the target SARS-CoV-2 NP was attached to the surface of the sensor via an antibody-antigen key-lock system followed the anchoring of HRP labeled anti-SARS-CoV-2 NP.

The HRP-labeled detection antibodies catalyzed the electrochemical oxidation of 3,3',5,5'-tetramethylbenzidine (TMB), creating a current signal that is used for the quantitative detection of SARS-CoV-2 NP. This immunosensor could successfully detect NP with the LOD of 50 plaque-forming units/mL (PFU/mL) and specificity of 100% in nasopharyngeal samples. In another report, Białobrzeska et al. investigated the label-free SARS-CoV-2 NP immunosensing performance based on a series of substrates, including Au, glassy carbon (GC), and boron-doped diamond electrode (BDD) (Figure 6b) [90].

For the immobilization of anti-SARS-CoV-2 NP, the Au electrode was modified with 4-aminothiophenol and glutaraldehyde, while both GC and BDD were sequentially modified with aryldiazonium and protein A-agarose affinity matrix. Thus, the anti-SARS-CoV-2 NP functionalized electrodes can selectively bind SARS-CoV-2 NP, which induces the variation in EIS responses for $[\text{Fe}(\text{CN})_6]^{3-/4-}$ redox probe with the variation of NP concentration.

The immunosensors enabled a fast detection of (less than 10 min) NP with the LOD of 0.227, 0.334, and 0.362 ng/mL for GC, BDD, and Au electrodes, respectively. Some other researcher utilized functionalized graphene, BiWO₆/Bi₂S₃/GCE, AuNPs/SCPE,

AuNPs/poly(aldehyde substituted thiophene) (Pthi-Ald)/indium-tin-oxide (ITO), Au nanostructured/SPCE, and screen-printed gold (SPG) electrodes for the effective immobilization of anti-SARS-CoV-2 NP and the subsequent binding of SARS-CoV-2 NP [62,91–95]. The corresponding analytical performance of these immunosensors is summarized in Table 4.

Table 4. Analytical performance of recently developed electrochemical biosensors for detecting SARS-CoV-2 NP.

Materials/Electrode	Detection Method	Receptors	Detection Medium	LOD	Linear Range	Ref.
Graphene	DPV	antibody	blood and saliva samples	-	-	[62]
COOH-SPCE	CA	antibody	PBS	50 PFU/mL	-	[89]
Au, GC, and BDD	EIS	antibody	PBS	0.227, 0.334, and 0.362 ng/mL, respectively	4.4 ng/mL–4.4 pg/mL	[90]
BiWO ₆ /Bi ₂ S ₃ /GC	DPV	antibody	PBS	3.00 fg/mL	0.01–1.00 pg/mL	[91]
AuNPs/SCPE	SWV	antibody	PBS	0.4 pg/mL	1.0 pg/mL–100 ng/mL	[92]
AuNPs/Pthi-Ald/ITO	EIS	antibody	PBS	0.48 fg/mL	0.0015 pg/mL–150 pg/mL	[93]
Au nanostructured/SPCE	EIS	antibody	PBS diluted saliva	6 pg/mL	0.01–100 ng/mL	[94]
SPG	CA	antibody	wholeserum	50 pg/mL	0–10 ng/mL	[95]
Au	DPV	aptamer	PBS	8.33 pg/mL	0–50 ng/mL	[96]
MEA	EIS	aptamer	PBS	fg/mL level	10 ⁻⁵ –10 ⁻² ng/mL	[97]
Au IDE	EIS	aptamer	PBS	0.389 fM	1 fM–100 pM	[98]
Au	DPV	aptamer	PBS	16.5 pg/mL	0.05–100 ng/mL	[99]
Au-TFE	DPV	MIP	nasopharyngeal	27 fM	0.22–333 fM	[100]
Au/graphene/SPCE	DPV	MIP	PBS	3.0 fM	10.0–200.0 fM	[101]

Similar to the development of electrochemical aptasensors for the detection of SARS-CoV-2 SP, aptamers were also used as a receptor for detecting SARS-CoV-2 NP. Tian et al. constructed a label-based electrochemical dual-aptamer sensor for SARS-CoV-2 NP biosensing, in which metal-organic frameworks (MIL-53(Al)) decorated with Au@Pt NPs, HRP, dual-aptamer, and hemin/G-quadruplex DNazymes (GQH DNzyme/dual-aptamer/HRP/Au@Pt/MIL-53) served as a nanoprobe for signal amplification (Figure 6c) [96]. The aptasensor was fabricated by the attachment of SARS-CoV-2 NP target-specific SH-functionalized dual aptamers onto an Au electrode surface via a self-assembled monolayer (SAM) mechanism.

Then, SARS-CoV-2 NP was anchored with the dual aptamer's follower by anchoring SARS-CoV-2 NP with GQH DNzyme/dual-aptamer/HRP/Au@Pt/MIL-53 nanoprobe to form a sandwich-type assay. This labeled nanoprobe induced the electrocatalytic oxidation of HQ in the presence of H₂O₂ and formed the basis of SARS-CoV-2 NP detection. The biosensor could selectively detect NP in a wide linear range with a low LOD (8.33 pg/mL).

Qi et al. reported another simple and ultra-trace NP aptasensor using a low-cost microelectrode array (MEA) chip [97]. This aptamer-modified MEA induced a variation of capacitance in the solid–liquid interface upon SARS-CoV-2 NP binding with a sensitivity of pM level. When integrated with an efficient microfluidic enrichment, the sensor could detect NP within 15 s in a wide linear range (10⁻⁵ to 10⁻² ng/mL) and low LOD (fg/mL level). Table 4 summarizes the analytical performance of some other reported electrochemical aptasensors for the detection of SARS-CoV-2 NP.

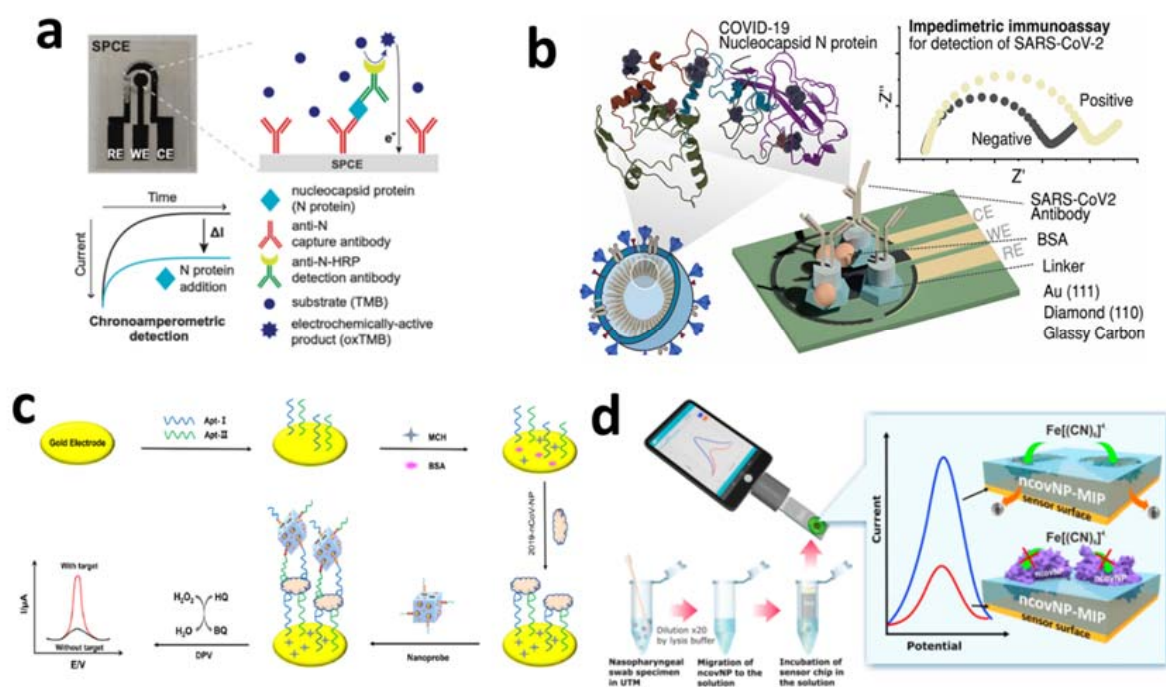


Figure 6. (a) Schematic illustration of the design and electrochemical responses of SCPE-based SARS-CoV-2 NP immunosensor (adapted with permission from ref. [89]). Copyright 2022 American Chemical Society. (b) Schematic illustration of the Au, GC, and BDD electrode-based EIS immunosensors for the detection of SARS-CoV-2 NP (adapted with permission from ref. [90]). Copyright 2022 Elsevier. (c) Schematic illustration of the development of aptasensor based on MIL-53(Al) decorated with Au@Pt NPs and enzymes for SARS-CoV-2 NP detection (adapted with permission from ref. [96]). Copyright 2021 Elsevier. (d) Schematic illustration of label-free MIP-based detection of SARS-CoV-2 NP (reprinted with permission from ref. [100]). Copyright 2021 Elsevier.

MIP is also used for the electrochemical detection of SARS-CoV-2 NP. In this process, a functional monomer is polymerized along with the target molecules and acts as a template. The subsequent removal of the target molecules from the template leaves behind the polymer along with binding sites of the same target molecule. Raziq et al. reported a portable poly-m-phenylenediamine (PmPD) based MIP for the detection of SARS-CoV-2 NP (Figure 6d) [100].

For the fabrication of the sensor, PmPD was electrochemically polymerized onto an Au-thin film electrode (Au-TFE). After imprinting the SARS-CoV-2 NP into the polymer matrix, the NP was removed from the SARS-CoV-2 NP-PmPD using 2-mercaptoethanol (2-ME) and 3,3'-dithiobis [sulfosuccinimidy] propionate]. This facilitates the rebounding of SARS-CoV-2 NP from the target solution and enables the label-free electrochemical detection of NP. The as-prepared sensor showed the capabilities of NP detection with a detection and quantification limit of 15 and 50 fM, respectively, in PBS.

Another MIP-based SARS-CoV-2 NP detection platform was developed by Zhang et al., in which poly-arginine (P-Arg) is used for the preparation of the SARS-CoV-2 NP-P-Arg MIP complex [101]. The sensor was fabricated by the immobilization of NP onto an Au/graphene/SPCE electrode followed by the electrochemical polymerization of Arg. This produced the SARS-CoV-2 NP-P-Arg MIP complex. Then, NP was removed from the MIP matrix for the selective binding of SARS-CoV-2 NP from the target analytes. The sensor could discriminate the redox responses of $[\text{Fe}(\text{CN})_6]^{3-/4-}$ by selectively binding NP with high sensitivity and low LOD (Table 4).

4.2.3. Detection of Whole Virus or Virus Particles

The biosensing of the SARS-CoV-2 virus using specific proteins requires external reagents and pre-/post-sample treatment, which can increase the detection cost and time. The development of POC detection systems for whole viral particles in biological samples with high sensitivity, selectivity, and accuracy is needed considering the high frequency of SARS-CoV-2 virus infections. Accordingly, few researchers have attempted to develop electrochemical biosensors for detecting whole viral particles. Seo et al. utilized a graphene-based FET immunoassay platform for screening SARS-CoV-2 viral particles based on the variation of current-voltage signals induced by the interaction between the anti-SARS-CoV-2 SP and viral particles (Figure 7a) [70].

The anti-SARS-CoV-2 SP functionalized graphene-based FET could selectively detect viral particles in culture medium and clinical samples with the LOD of 1.6×10^1 pfu/mL and 2.42×10^2 copies/mL, respectively. Recently, Yousefi et al. constructed a reagent-free electrochemical sensor for whole virus detection using a standalone electrode chip (Figure 7b) [102]. The Au-based sensor chip was modified with a negatively-charged ferrocene redox labeled DNA. This functionalized sensor having an analyte-binding antibody could effectively bind the viral particles and form the complex.

Upon applying a positive potential to the sensor surface, the complex is attracted electrostatically to the electrode surface due to the negative charges of the DNA linker. This facilitates the ferrocene label to come into close contact with the electrode, thus, electron transfer occurs, and ferrocene is oxidized. The electron transfer kinetic response of ferrocene oxidation was determined via chrono-amperometry to analyze the sensing performance.

The sensor is capable of screening SARS-CoV-2 virus particles within 5 min in unprocessed patient saliva samples with high specificity and selectivity. In another report, Sukjee et al. constructed an electrochemical MIP-based biosensor for detecting SARS-CoV-2 virus particles in the environmental samples (Figure 7c) [103]. The MIP for capturing virus particles was constructed using polymer-GO composite, which was used to prepare MIP-SARS-CoV-2 complexes. Upon removing the SARS-CoV-2 viral particles from the complex using HCl, the MIP was used to modify SPCE for the label-free electrochemical detection of virus particles. The rebinding of viral particles onto the sensor surface showed a low LOD (0.1 fM) in buffer solution and wastewater spiked with SARS-CoV-2.

4.3. Electrochemical Nucleic Acid-Based Detection of SARS-CoV-2 Virus

Electrochemical biosensing for the diagnosis of COVID-19 infection is mainly based on the serological test, which detects the presence of antibodies and antigens (viral structural proteins and whole viral particles). The clinical efficacy of antibody-based biosensors for detecting SARS-CoV-2 is restricted due to the possibility of false-negative results at the early stage of infection. This can be attributed that antibody generation in human body fluids may take several days to weeks to develop a detectable response in COVID-19 patients after starting to show the symptoms. Rapid antigen tests for SARS-CoV-2 are generally less sensitive than NA-based tests.

Therefore, for the accurate diagnosis of COVID-19 infection, NA testing is the most reliable method. Considering these issues and limitations of the RT-PCR method, electrochemical biosensors for screening SARS-CoV-2 NA were also developed to improve the clinical efficacy and reliability of COVID-19 diagnosis [104–107]. Kong et al. constructed a NA assay using a Y-shaped dual DNA probe-modified graphene FET that could simultaneously target ORF1ab and N genes of SARS-CoV-2 NA (Figure 8a) [105].

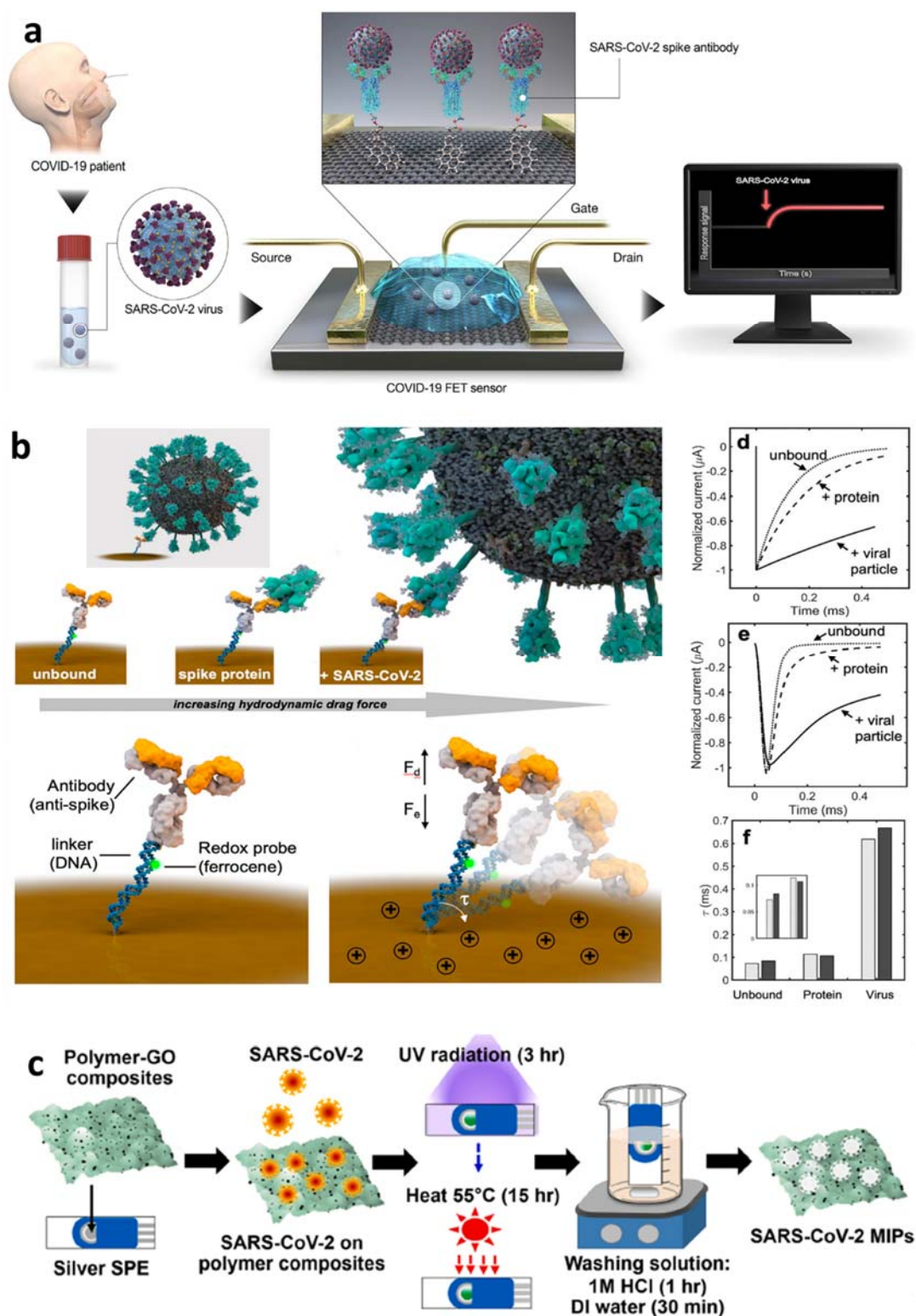


Figure 7. (a) Schematic illustration of the design of graphene-based FET sensors for the detection of viral particles (adapted with permission from ref. [70]). Copyright 2020 American Chemical Society. (b) Schematic representation of reagent-free viral particles sensing platform based on the monitoring of the electron transport kinetics of DNA–viral antibody complex (reprinted with permission from ref. [102]). Copyright 2021 American Chemical Society. (c) Schematic illustration of the fabrication of polymer-GO-based MIPs for selective binding of SARS-CoV-2 viral particles (reprinted with permission from ref. [103]). Copyright 2022 Elsevier.

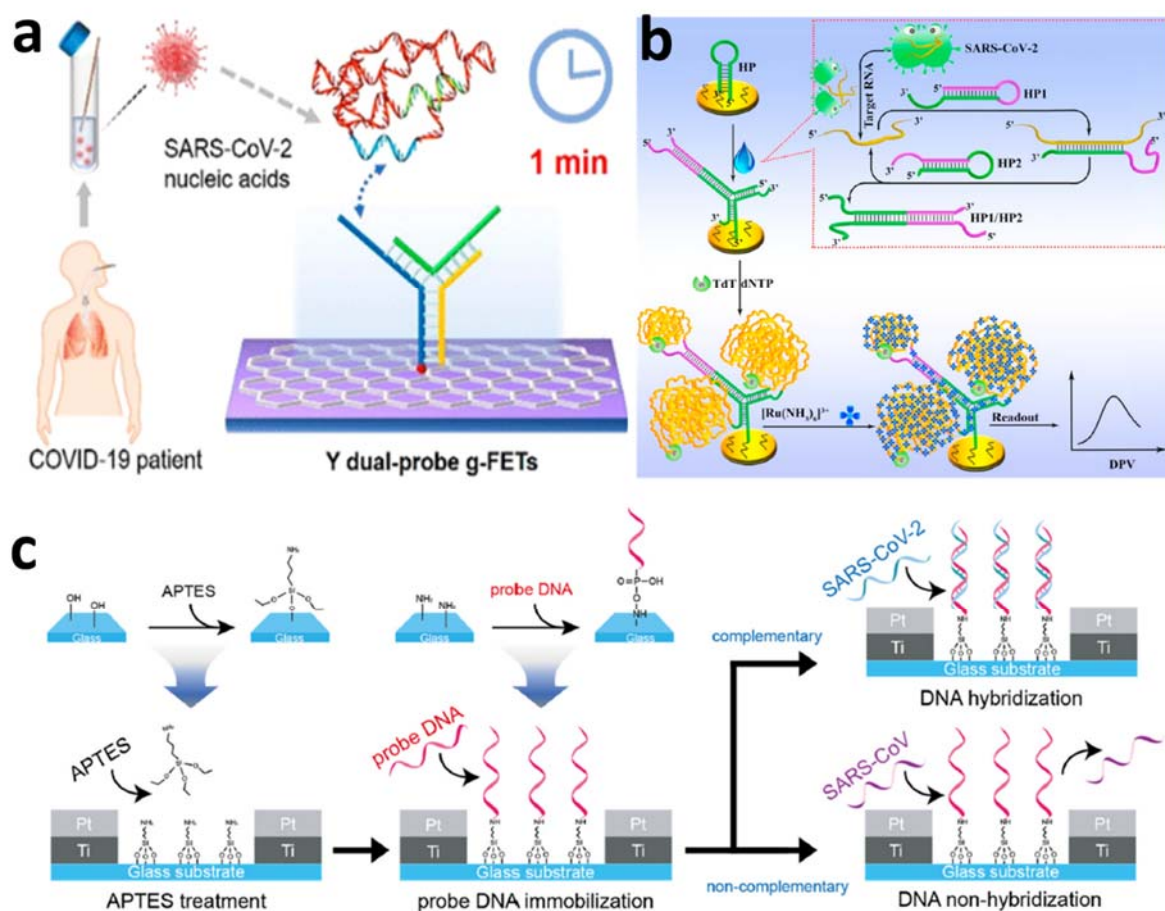


Figure 8. (a) Schematic of the Y-dual probe/graphene-based FET biosensor for SARS-CoV-2 NA detection (adapted from ref. [105]). Copyright 2021 American Chemical Society. (b) Schematic of the operation principle of SARS-CoV-2 NA monitoring by combining the signal amplification strategy (reproduced from ref. [106]). Copyright 2021 Elsevier. (c) Schematic of the fabrication of interdigitated platinum/titanium electrodes treated with APTES followed by probe DNA immobilization and the hybridization of target complementary DNA for SARS-CoV-2 NA detection (reproduced from ref. [107]). Copyright 2021 Elsevier.

The simultaneous binding of the ORF1ab and N gene at the sensor probe induced a higher recognition ratio with the LOD down to 3 copies in 100 μ L of testing solution. The biosensor was also capable to detect NA within \sim 1 min without the necessity of NA extraction and amplification, and thus could be used as a comprehensive testing method for COVID-19 screening.

Peng et al. constructed a SARS-CoV-2 RNA biosensor based on a hairpin probe (oligonucleotide sequence) modified Au electrode (Figure 8b) [106]. The introduction of SARS-CoV-2 RNA triggers the catalytic hairpin assembly circuit and initiates terminal deoxynucleotidyl transferase (dNTP)-mediated DNA polymerization with a large number of long single-stranded DNA products. This negatively charged DNA polymer electrostatically binds the positively charged $Ru(NH_3)_6^{3+}$ redox probe and forms the basis of electrochemical SARS-CoV-2 RNA detection.

The sensor showed excellent capabilities of SARS-CoV-2 RNA detection with a LOD of 26 fM. In another report, Hwang et al. prepared an interdigitated Pt/Ti electrode on the glass substrate for detecting SARS-CoV-2 NA (Figure 8c) [107]. The 3-aminopropyltriethoxysilane (APTES)-modified glass substrate based interdigitated Pt/Ti electrode was used to immobilize probe DNA via phosphoramidate linkage. The hybridization of complementary

SARS-CoV-2 cDNA induced the change in capacitance and enabled the detection of SARS-CoV-2 NA with high sensitivity (0.843 nF/nM).

5. Conclusions, Challenges, and Future Perspectives

This review comprehensively discussed the advances in the development of electrochemical biosensors and immuno-sensors for detecting the SARS-CoV-2 virus. This includes the detection of SARS-CoV-2 structural proteins (spike protein and nucleocapsid protein), nucleic acid, and antibodies generated after COVID-19 infection. Both label-free and label-based electrochemical detection strategies were described by developing novel electrode materials and bio-receptors, such as antibodies, aptamers, molecularly imprinted polymers, and angiotensin-converting enzyme 2. This review also briefly highlighted the structure of the SARS-CoV-2 virus along with the functions of structural proteins and the strategies for the detection of this virus.

During the preparation of this review, the author found that researchers, scientists, and academicians from different countries of the world have made substantial efforts to construct electrochemical biosensors for COVID-19 infection diagnosis by developing novel strategies, detection methods, electrode materials, and electrode fabrication processes. Accordingly, rapid, sensitive, selective, and low-cost electrochemical biosensors for SARS-CoV-2 screening were successfully achieved within a short time.

However, some challenges still exist for the electrochemical biosensing of COVID-19 with high accuracy and reliability due to the commonly observed false positive/negative signals. This is because most of the developed electrochemical biosensors for COVID-19 diagnosis are based on single biomarker (antigen, antibody, and nucleic acid) monitoring, which can be combined into a multiplexed detection system for targeting multiple biomarkers for the reliable and accurate diagnosis of COVID-19.

The other common challenges for the commercialization of electrochemical SARS-CoV-2 biosensors are the low stability and the signal reproducibility within the error range. This can be achieved by developing novel and stable signal amplifications materials and receptors, such as phage display antibodies instead of conventional monoclonal antibodies and nanomaterial-based receptors. It is noteworthy that some researchers developed MIP-type nanomaterials for electrochemical SARS-CoV-2 detection with high stability and low LOD (fM) compared to the protein-based sensors [100,101].

Since SARS-CoV-2 is highly contagious, to minimize the rate of virus infection and its associated fatality, it is desirable to diagnose COVID-19 by developing electrochemical biosensors other than for structural proteins, nucleic acid, and the whole virus. COVID-19 infection can release reactive oxygen species (ROS) from damaged mitochondria [108] and significantly increase the concentration of CRP, procalcitonin, and ferritin in the biological fluids of patients [109]. Thus, it is desirable to develop electrochemical sensors/biosensors for detecting ROS, CRP, procalcitonin, and ferritin to diagnose COVID-19 infection.

Finally, the high infection and fatality rate of the SARS-CoV-2 virus pushes researchers, scientists, and industrialists to develop a reliable and effective electrochemical biosensor. Accordingly, the research for the development of electrochemical biosensors to diagnose COVID-19 is advancing at an unparalleled pace. Soon, we might observe the commercial electrochemical biosensors with low-cost, POC and PON testing ability, and high reliability, along with the remote sensing capacity for diagnosing COVID-19 to serve mankind in overcoming the difficult situation that the world is currently facing.

Funding: M. M. Rahman thanks Konkuk University for the financial support (Project # 2022-A019-0142).

Institutional Review Board Statement: Not applicable.

Informed Consent Statement: Not applicable.

Data Availability Statement: Not applicable.

Acknowledgments: This paper was supported by Konkuk University in 2022.

Conflicts of Interest: The authors declare no conflict of interest.

References

1. Hu, B.; Guo, H.; Zhou, P.; Shi, Z.-L. Characteristics of SARS-CoV-2 and COVID-19. *Nat. Rev. Microbiol.* **2021**, *19*, 141–154. [[CrossRef](#)] [[PubMed](#)]
2. Feng, W.; Zong, W.; Wang, F.; Ju, S. Severe acute respiratory syndrome coronavirus 2 (SARS-CoV-2): A review. *Mol. Cancer* **2020**, *19*, 100. [[CrossRef](#)] [[PubMed](#)]
3. Cucinotta, D.; Vanelli, M. WHO Declares COVID-19 a Pandemic. *Acta Biomed.* **2020**, *91*, 157–160. [[PubMed](#)]
4. COVID-19 Coronavirus Pandemic. Available online: <https://www.worldometers.info/coronavirus/> (accessed on 29 May 2022).
5. Available online: <https://www.axios.com/2022/04/13/world-covid-cases-surpass-500-million> (accessed on 29 May 2022).
6. Harvey, W.T.; Carabelli, A.M.; Jackson, B.; Gupta, R.K.; Thomson, E.C.; Harrison, E.M.; Ludden, C.; Reeve, R.; Rambaut, A.; COVID-19 Genomics UK (COG-UK) Consortium; et al. SARS-CoV-2 variants, spike mutations and immune escape. *Nat. Rev. Microbiol.* **2021**, *19*, 409–424. [[CrossRef](#)]
7. Taleghani, N.; Taghipour, F. Diagnosis of COVID-19 for controlling the pandemic: A review of the state-of-the-art. *Biosens. Bioelectron.* **2021**, *174*, 112830. [[CrossRef](#)]
8. Yüce, M.; Filiztekin, E.; Özkaya, K.G. COVID-19 diagnosis-a review of current methods. *Biosens. Bioelectron.* **2021**, *172*, 112752. [[CrossRef](#)]
9. Kaushik, A.K.; Dhau, J.S.; Gohel, H.; Mishra, Y.K.; Kateb, B.; Kim, N.-Y.; Goswami, D.Y. Electrochemical SARS-CoV-2 Sensing at Point-of-Care and Artificial Intelligence for Intelligent COVID-19 Management. *ACS Appl. Bio. Mater.* **2020**, *3*, 7306–7325. [[CrossRef](#)]
10. Kashir, J.; Yaquinnuddin, A. Loop mediated isothermal amplification (LAMP) assays as a rapid diagnostic for COVID-19. *Med. Hypotheses* **2020**, *141*, 109786. [[CrossRef](#)]
11. Sun, Y.; Yu, L.; Liu, C.; Ye, S.; Chen, W.; Li, D.; Huang, W. One-tube SARS-CoV-2 detection platform based on RT-RPA and CRISPR/Cas12a. *J. Transl. Med.* **2021**, *19*, 74. [[CrossRef](#)]
12. Jiao, J.; Duan, C.; Xue, L.; Liu, Y.; Sun, W.; Xiang, Y. DNA nanoscaffold-based SARS-CoV-2 detection for COVID-19 diagnosis. *Biosens. Bioelectron.* **2020**, *167*, 112479. [[CrossRef](#)]
13. Serebrennikova, K.V.; Byzova, N.A.; Zherdev, A.V.; Khlebtsov, N.G.; Khlebtsov, B.N.; Biketov, S.F.; Dzantiev, B.B. Lateral Flow Immunoassay of SARS-CoV-2 Antigen with SERS-Based Registration: Development and Comparison with Traditional Immunoassays. *Biosensors* **2021**, *11*, 510. [[CrossRef](#)] [[PubMed](#)]
14. Alharbi, S.A.; Almutairi, A.Z.; Jan, A.A.; Alkhalify, A.M. Enzyme-Linked Immunosorbent Assay for the Detection of Severe Acute Respiratory Syndrome Coronavirus 2 (SARS-CoV-2) IgM/IgA and IgG Antibodies Among Healthcare Workers. *Cureus* **2020**, *12*, e10285. [[CrossRef](#)] [[PubMed](#)]
15. Infantino, M.; Grossi, V.; Lari, B.; Bambi, R.; Perri, A.; Manneschi, M.; Terenzi, G.; Liotti, I.; Ciotta, G.; Taddei, C.; et al. Diagnostic accuracy of an automated chemiluminescent immunoassay for anti-SARS-CoV-2 IgM and IgG antibodies: An Italian experience. *J. Med. Virol.* **2020**, *92*, 1–5. [[CrossRef](#)] [[PubMed](#)]
16. Drobysh, M.; Ramanaviciene, A.; Viter, R.; Chen, C.-F.; Samukaite-Bubniene, U.; Ratautaite, V.; Ramanavicius, A. Biosensors for the Determination of SARS-CoV-2 Virus and Diagnosis of COVID-19 Infection. *Int. J. Mol. Sci.* **2022**, *23*, 666. [[CrossRef](#)]
17. Jiang, C.; Mu, X.; Du, B.; Tong, Z. A review of electrochemical biosensor application in the detection of the SARS-CoV-2. *Micro Nano Lett.* **2022**, *17*, 49–58. [[CrossRef](#)]
18. Adeel, M.; Asif, K.; Rahman, M.M.; Daniele, S.; Canzonieri, V.; Rizzolio, F. Glucose Detection Devices and Methods Based on Metal–Organic Frameworks and Related Materials. *Adv. Funct. Mater.* **2021**, *31*, 2106023. [[CrossRef](#)]
19. Rahman, M.M.; Lopa, N.S.; Lee, J.-J. Advances in electrochemical aptasensing for cardiac biomarkers. *Bull. Korean Chem. Soc.* **2022**, *43*, 51–68. [[CrossRef](#)]
20. Adeel, M.; Rahman, M.M.; Caligiuri, I.; Canzonieri, V.; Rizzolio, F.; Daniele, S. Recent advances of electrochemical and optical enzyme-free glucose sensors operating at physiological conditions. *Biosens. Bioelectron.* **2020**, *165*, 112331. [[CrossRef](#)]
21. Lopa, N.S.; Rahman, M.M.; Ahmed, F.; Ryu, T.; Sutradhar, S.C.; Lei, J.; Kim, J.; Kim, D.H.; Lee, Y.H.; Kim, W. Simple, low-cost, sensitive and label-free aptasensor for the detection of cardiac troponin I based on a gold nanoparticles modified titanium foil. *Biosens. Bioelectron.* **2019**, *126*, 381–388. [[CrossRef](#)]
22. Rahman, M.M.; Lopa, N.S.; Kim, Y.J.; Choi, D.-K.; Lee, J.-J. Label-Free DNA Hybridization Detection by Poly(Thionine)-Gold Nanocomposite on Indium Tin Oxide Electrode. *J. Electrochem. Soc.* **2016**, *163*, B153–B157. [[CrossRef](#)]
23. Kumar, N.; Shetti, N.P.; Jagannath, S.; Aminabhavi, T.M. Electrochemical sensors for the detection of SARS-CoV-2 virus. *Chem. Eng. J.* **2022**, *430*, 132966. [[CrossRef](#)] [[PubMed](#)]
24. Madhurantakam, S.; Muthukumar, S.; Prasad, S. Emerging Electrochemical Biosensing Trends for Rapid Diagnosis of COVID-19 Biomarkers as Point-of-Care Platforms: A Critical Review. *ACS Omega* **2022**, *7*, 12467–12473. [[CrossRef](#)] [[PubMed](#)]
25. Bar-On, Y.M.; Flamholz, A.; Phillips, R.; Milo, R. SARS-CoV-2 (COVID-19) by the numbers. *eLife* **2020**, *9*, e57309. [[CrossRef](#)] [[PubMed](#)]
26. Malik, Y.A. Properties of coronavirus and SARS-CoV-2. *Malays. J. Pathol.* **2020**, *42*, 3–11. [[PubMed](#)]
27. Raj, R. Analysis of non-structural proteins, NSPs of SARS-CoV-2 as targets for computational drug designing. *Biochem. Biophys. Rep.* **2021**, *25*, 100847. [[CrossRef](#)] [[PubMed](#)]

28. Chang, C.-K.; Hou, M.-H.; Chang, C.-F.; Hsiao, C.-D.; Huang, T.-H. The SARS coronavirus nucleocapsid protein—Forms and functions. *Antivir. Res.* **2014**, *103*, 39–50. [CrossRef]
29. McBride, R.; Zyl, M.V.; Fielding, B.C. The Coronavirus Nucleocapsid Is a Multifunctional Protein. *Viruses* **2014**, *6*, 2991–3018. [CrossRef]
30. Huang, Y.; Yang, C.; Xu, X.-F.; Xu, W.; Liu, S.-W. Structural and functional properties of SARS-CoV-2 spike protein: Potential antiviral drug development for COVID-19. *Acta Pharmacol. Sin.* **2020**, *41*, 1141–1149. [CrossRef]
31. Sternberg, A.; Naujokat, C. Structural features of coronavirus SARS-CoV-2 spike protein: Targets for vaccination. *Life Sci.* **2020**, *257*, 118056. [CrossRef]
32. Schoeman, D.; Fielding, B.C. Coronavirus envelope protein: Current knowledge. *Viol. J.* **2019**, *16*, 69. [CrossRef]
33. Boson, B.; Legros, V.; Zhou, B.; Siret, E.; Mathieu, C.; Cosset, F.-L.; Lavillette, D.; Denolly, S. The SARS-CoV-2 envelope and membrane proteins modulate maturation and retention of the spike protein, allowing assembly of virus-like particles. *J. Biol. Chem.* **2021**, *296*, 100111. [CrossRef] [PubMed]
34. Thomas, S. The Structure of the Membrane Protein of SARS-CoV-2 Resembles the Sugar Transporter SemiSWEET. *Pathog. Immun.* **2020**, *5*, 342–363. [CrossRef] [PubMed]
35. Kontou, P.I.; Braliou, G.G.; Dimou, N.L.; Nikolopoulos, G.; Bagos, P.G. Antibody Tests in Detecting SARS-CoV-2 Infection: A Meta-Analysis. *Diagnostics* **2020**, *10*, 319. [CrossRef] [PubMed]
36. Kim, Y.J.; Rahman, M.M.; Lee, J.-J. Ultrasensitive and label-free detection of annexin A3 based on quartz crystal microbalance. *Sens. Actuators B Chem.* **2013**, *177*, 172–177. [CrossRef]
37. Ruiz de Eguilaz, M.; Cumba, L.R.; Forster, R.J. Electrochemical detection of viruses and antibodies: A mini review. *Electrochem. Commun.* **2020**, *16*, 106762. [CrossRef]
38. Ozer, T.; Geiss, B.J.; Henry, C.S. Review-Chemical and Biological Sensors for Viral Detection. *J. Electrochem. Soc.* **2020**, *167*, 037523. [CrossRef]
39. Koyappayil, A.; Lee, M.-H. Ultrasensitive Materials for Electrochemical Biosensor Labels. *Sensors* **2021**, *21*, 89. [CrossRef]
40. Ehsan Shabani, E.; Dowlatshahi, S.; Abdekhodaie, M.J. Laboratory detection methods for the human coronaviruses. *Eur. J. Clin. Microbiol. Infect. Dis.* **2021**, *40*, 225–246. [CrossRef]
41. Coronavirus Disease 2019 (COVID-19) Emergency Use Authorizations for Medical Devices FDA. 2020. Available online: <https://www.fda.gov/medical-devices/emergency-use-authorizations-medical-devices/coronavirus-disease-2019-covid-19-emergency-use-authorizations-medical-devices> (accessed on 29 May 2022).
42. Rahman, M.M.; Kim, Y.J.; Lee, J.-J. Label-Free Detection of DNA Hybridization by Using Charge Perturbation on Poly(thionine)-Modified Glassy Carbon and Gold Electrodes. *J. Electrochem. Soc.* **2015**, *162*, B159–B162. [CrossRef]
43. Rahman, M.M.; Kim, Y.J.; Lee, J.-J. Sensitivity Control of Label-free DNA Hybridization Detection Based on Poly(thionine)-Modified Glassy Carbon and Gold Electrodes. *Bull. Korean Chem. Soc.* **2017**, *38*, 27–32. [CrossRef]
44. Falasca, F.; Sciardra, I.; Di Carlo, D.; Gentile, M.; Deales, A.; Antonelli, G.; Turriziani, O. Detection of SARS-CoV N2 gene: Very low amounts of viral RNA or false positive? *J. Clin. Virol.* **2020**, *133*, 104660. [CrossRef] [PubMed]
45. Xu, L.; Li, D.; Ramadan, S.; Li, Y.; Klein, N. Facile biosensors for rapid detection of COVID-19. *Biosens. Bioelectron.* **2020**, *170*, 112673. [CrossRef]
46. Pan, Y.; Li, X.; Yang, G.; Fan, J.; Tang, Y.; Zhao, J.; Long, X.; Guo, S.; Zhao, Z.; Liu, Y.; et al. Serological immunochromatographic approach in diagnosis with SARSCoV-2 infected COVID-19 patients. *J. Infect.* **2020**, *81*, e28–e32. [CrossRef] [PubMed]
47. Burrell, C.J.; Howard, C.R.; Murphy, F.A. Chapter 6-Adaptive Immune Responses to Infection; In Fenner and White's Medical Virology, 5th ed.; Burrell, C.J., Howard, C.R., Murphy, F.A., Eds.; Academic Press: London, UK, 2017; pp. 65–76.
48. Casali, P. IgM. In *Encyclopedia of Immunology*, 2nd ed.; Delves, P.J., Ed.; Elsevier: Oxford, UK, 1998; pp. 1212–1217.
49. Neumann, F.; Rose, R.; Römpke, J.; Grobe, O.; Lorentz, T.; Fickenscher, H.; Krumbholz, A. Development of SARS-CoV-2 Specific IgG and Virus-Neutralizing Antibodies after Infection with Variants of Concern or Vaccination. *Vaccines* **2021**, *9*, 700. [CrossRef] [PubMed]
50. Ge, C.-Y.; Rahman, M.M.; Zhang, W.; Lopa, N.S.; Jin, L.; Yoon, S.; Jang, H.; Xu, G.-R.; Kim, W. An Electrochemical Immunosensor Based on a Self-Assembled Monolayer Modified Electrode for Label-Free Detection of α -Synuclein. *Sensors* **2020**, *20*, 617. [CrossRef] [PubMed]
51. Adeel, M.; Rahman, M.M.; Lee, J.-J. Label-free aptasensor for the detection of cardiac biomarker myoglobin based on gold nanoparticles decorated boron nitride nanosheets. *Biosens. Bioelectron.* **2019**, *126*, 143–150. [CrossRef]
52. Rahman, M.M.; Liu, D.; Lopa, N.S.; Baek, J.-B.; Nam, C.-H.; Lee, J.-J. Effect of the carboxyl functional group at the edges of graphene on the signal sensitivity of dopamine detection. *J. Electroanal. Chem.* **2021**, *898*, 115628. [CrossRef]
53. Rahman, M.M.; Lopa, N.S.; Ju, M.J.; Lee, J.-J. Highly sensitive and simultaneous detection of dopamine and uric acid at graphene nanoplatelet-modified fluorine-doped tin oxide electrode in the presence of ascorbic acid. *J. Electroanal. Chem.* **2017**, *792*, 54–60. [CrossRef]
54. Yakoh, A.; Pimpitak, U.; Rengpipat, S.; Hirankarn, N.; Chailapakul, N.; Chaiyo, S. Paper-Based Electrochemical Biosensor for Diagnosing COVID-19: Detection of SARS-CoV-2 Antibodies and Antigen. *Biosens. Bioelectron.* **2021**, *176*, 112912. [CrossRef]
55. Ali, M.A.; Hu, C.; Zhang, F.; Jahan, S.; Yuan, B.; Saleh, M.S.; Gao, S.-J.; Panat, R. N protein-based ultrasensitive SARS-CoV-2 antibody detection in seconds via 3D nanoprinted, microarchitected array electrodes. *J. Med. Virol.* **2022**, *94*, 2067–2078. [CrossRef]

56. Ali, M.A.; Hu, C.; Jahan, S.; Yuan, B.; Saleh, M.S.; Ju, E.; Gao, S.-J.; Panat, R. Sensing of COVID-19 Antibodies in Seconds via Aerosol Jet Nanoprinted Reduced-Graphene-Oxide-Coated 3D Electrodes. *Adv. Mater.* **2021**, *33*, 2006647. [CrossRef] [PubMed]
57. Hashemi, S.A.; Bahrani, S.; Mousavi, S.M.; Omidifar, N.; Behbahan, N.G.G.; Arjmand, M.; Ramakrishna, S.; Lankarani, K.B.; Moghadami, M.; Shokripour, M.; et al. Ultra-precise label-free nanosensor based on integrated graphene with Au nanostars toward direct detection of IgG antibodies of SARS-CoV-2 in blood. *J. Electroanal. Chem.* **2021**, *894*, 115341. [CrossRef] [PubMed]
58. Li, X.; Qin, Z.; Fu, H.; Li, T.; Peng, R.; Li, Z.; Rini, J.M.; Liu, X. Enhancing the performance of paper-based electrochemical impedance spectroscopy nanobiosensors: An experimental approach. *Biosens. Bioelectron.* **2021**, *177*, 112672. [CrossRef] [PubMed]
59. Ameku, W.A.; Provance, D.W.; Morel, C.M.; De-Simone, S.G. Rapid Detection of Anti-SARS-CoV-2 Antibodies with a Screen-Printed Electrode Modified with a Spike Glycoprotein Epitope. *Biosensors* **2022**, *12*, 272. [CrossRef] [PubMed]
60. Tran, V.V.; Tran, N.H.T.; Hwang, H.S.; Chang, M. Development strategies of conducting polymer-based electrochemical biosensors for virus biomarkers: Potential for rapid COVID-19 detection. *Biosens. Bioelectron.* **2021**, *182*, 113192. [CrossRef]
61. Rashed, M.Z.; Kopechek, J.A.; Priddy, M.C.; Hamorsky, K.T.; Palmer, K.E.; Mittal, N.; Valdez, J.; Flynn, J.; Williams, S.J. Rapid detection of SARS-CoV-2 antibodies using electrochemical impedance-based detector. *Biosens. Bioelectron.* **2021**, *171*, 112709. [CrossRef]
62. Torrente-Rodríguez, R.M.; Lukas, H.; Tu, J.; Min, J.; Yang, Y.; Xu, C.; Rossiter, H.B.; Gao, W. SARS-CoV-2 RapidPlex: A Graphene-Based Multiplexed Telemedicine Platform for Rapid and Low-Cost COVID-19 Diagnosis and Monitoring. *Matter* **2020**, *3*, 1981–1998. [CrossRef]
63. Peng, R.; Pan, Y.; Li, Z.; Qin, Z.; Rini, J.M.; Liu, X. SPEEDS: A portable serological testing platform for rapid electrochemical detection of SARS-CoV-2 antibodies. *Biosens. Bioelectron.* **2022**, *197*, 113762. [CrossRef]
64. Zhang, Z.; Wang, X.; Wei, X.; Zheng, S.W.; Lenhart, B.J.; Xu, P.; Li, J.; Pan, J.; Albrecht, H.; Liu, C. Multiplex quantitative detection of SARS-CoV-2 specific IgG and IgM antibodies based on DNA-assisted nanopore sensing. *Biosens. Bioelectron.* **2021**, *181*, 113134. [CrossRef]
65. Rahmati, Z.; Roushani, M.; Hosseini, H.; Choobin, H. An electrochemical immunosensor using SARS-CoV-2 spike protein-nickel hydroxide nanoparticles bio-conjugate modified SPCE for ultrasensitive detection of SARS-CoV-2 antibodies. *Microchem. J.* **2021**, *170*, 106718. [CrossRef]
66. Find. Test Directory, FIND. (n.d.). Available online: <https://www.finddx.org/test-directory/> (accessed on 25 May 2022).
67. Abdelhamid, H.N.; Badr, G. Nanobiotechnology as a platform for the diagnosis of COVID-19: A review. *Nanotechnol. Environ. Eng.* **2021**, *6*, 19. [CrossRef]
68. Liu, G.; Rusling, J.F. COVID-19 antibody tests and their limitations. *ACS Sens.* **2021**, *6*, 593–612. [CrossRef] [PubMed]
69. Adeel, M.; Asif, K.; Canzonieri, V.; Barai, H.S.; Rahman, M.M.; Daniele, S.; Rizzolio, F. Controlled, partially exfoliated, self-supported functionalized flexible graphitic carbon foil for ultrasensitive detection of SARS-CoV-2 spike protein. *Sens. Actuators B Chem.* **2022**, *359*, 131591. [CrossRef] [PubMed]
70. Seo, G.; Lee, G.; Kim, M.J.; Baek, S.-H.; Choi, M.; Ku, K.B.; Lee, C.-S.; Jun, S.; Park, D.; Kim, H.G.; et al. Rapid Detection of COVID-19 Causative Virus (SARS-CoV-2) in Human Nasopharyngeal Swab Specimens Using Field-Effect Transistor- Based Biosensor. *ACS Nano* **2020**, *14*, 5135–5142. [CrossRef] [PubMed]
71. Malla, P.; Liao, H.-P.; Liu, C.-H.; Wu, W.-C.; Sreearunothai, P. Voltammetric biosensor for coronavirus spike protein using magnetic bead and screen-printed electrode for point-of-care diagnostics. *Microchim. Acta* **2022**, *189*, 168. [CrossRef] [PubMed]
72. Idili, A.; Parolo, C.; Alvarez-Diduk, R.; Merkoç, A. Rapid and Efficient Detection of the SARS-CoV-2 Spike Protein Using an Electrochemical Aptamer-Based Sensor. *ACS Sens.* **2021**, *6*, 3093–3101. [CrossRef]
73. Curti, F.; Fortunati, S.; Knoll, W.; Giannetto, M.; Corradini, R.; Bertucci, A.; Careri, M. A Folding-Based Electrochemical Aptasensor for the Single-Step Detection of the SARS-CoV-2 Spike Protein. *ACS Appl. Mater. Interfaces* **2022**, *14*, 19204–19211. [CrossRef]
74. Lan, J.; Ge, J.; Yu, J.; Shan, S.; Zhou, H.; Fan, S.; Zhang, Q.; Shi, X.; Wang, Q.; Zhang, L.; et al. Structure of the SARS-CoV-2 spike receptor-binding domain bound to the ACE2 receptor. *Nature* **2020**, *581*, 215–220. [CrossRef]
75. Vezza, V.J.; Butterworth, A.; Lasserre, P.; Blair, E.O.; MacDonald, A.; Hannah, S.; Rinaldi, C.; Hoskisson, P.A.; Ward, A.C.; Longmuir, A.; et al. An electrochemical SARS-CoV-2 biosensor inspired by glucose test strip manufacturing processes. *Chem. Commun.* **2021**, *57*, 3704–3707. [CrossRef]
76. Nascimento, E.D.; Fonseca, W.T.; de Oliveira, T.R.; de Correia, C.R.S.T.B.; Faça, V.M.; de Moraes, B.P.; Silvestrini, V.C.; Pott-Junior, H.; Teixeira, F.R.; Faria, R.C. COVID-19 diagnosis by SARS-CoV-2 Spike protein detection in saliva using an ultrasensitive magneto-assay based on disposable electrochemical sensor. *Sens. Actuators B Chem.* **2022**, *353*, 131128. [CrossRef]
77. Pan, J.; Chen, W.; Ma, Y.; Pan, G. Molecularly imprinted polymers as receptor mimics for selective cell recognition. *Chem. Soc. Rev.* **2018**, *47*, 5574–5587. [CrossRef] [PubMed]
78. Yano, K.; Karube, I. Molecularly imprinted polymers for biosensor applications. *Trends Anal. Chem.* **1999**, *18*, 199–204. [CrossRef]
79. Ayankojo, A.G.; Boroznjak, R.; Reut, J.; Opik, A.; Syritski, V. Molecularly imprinted polymer based electrochemical sensor for quantitative detection of SARS-CoV-2 spike protein. *Sens. Actuators B Chem.* **2022**, *353*, 131160. [CrossRef] [PubMed]
80. Soares, J.C.; Soares, A.C.; Angelim, M.K.S.C.; Proença-Modena, J.L.; Moraes-Vieira, P.M.; Mattoso, L.H.C.; Oliveira, O.N., Jr. Diagnostics of SARS-CoV-2 infection using electrical impedance spectroscopy with an immunosensor to detect the spike protein. *Talanta* **2022**, *239*, 123076. [CrossRef] [PubMed]

81. Liustrovaite, V.; Drobysh, M.; Rucinskiene, A.; Baradoke, A.; Ramanaviciene, A.; Plikusiene, I.; Samukaite-Bubniene, U.; Viter, R.; Chen, C.-F.; Ramanavic, A. Towards an Electrochemical Immunosensor for the Detection of Antibodies against SARS-CoV-2 Spike Protein. *J. Electrochem. Soc.* **2022**, *169*, 037523. [[CrossRef](#)]
82. Rahmati, Z.; Roushani, M.; Hosseini, H.; Choobin, H. Electrochemical immunosensor with Cu₂O nanocube coating for detection of SARS-CoV-2 spike protein. *Microchim. Acta* **2021**, *188*, 105. [[CrossRef](#)]
83. Lasserre, P.; Balansethupathy, B.; Vezza, V.J.; Butterworth, A.; Macdonald, A.; Blair, E.O.; McAteer, L.; Hannah, S.; Ward, A.C.; Hoskisson, P.A.; et al. SARS-CoV-2 Aptasensors Based on Electrochemical Impedance Spectroscopy and Low-Cost Gold Electrode Substrates. *Anal. Chem.* **2022**, *94*, 2126–2133. [[CrossRef](#)]
84. Abrego-Martinez, J.C.; Jafari, M.; Chergui, S.; Pavel, C.; Che, D.; Siaj, M. Aptamer-based electrochemical biosensor for rapid detection of SARS-CoV-2: Nanoscale electrode-aptamer-SARS-CoV-2 imaging by photo-induced force microscopy. *Biosens. Bioelectron.* **2022**, *195*, 113595. [[CrossRef](#)]
85. Tabrizi, M.A.; Acedo, P. An Electrochemical Impedance Spectroscopy-Based Aptasensor for the Determination of SARS-CoV-2-RBD Using a Carbon Nanofiber–Gold Nanocomposite Modified Screen-Printed Electrode. *Biosensors* **2022**, *12*, 142. [[CrossRef](#)]
86. Ratautaite, V.; Boguzaitė, R.; Brazys, E.; Ramanaviciene, A.; Ciplys, E.; Juozapaitis, M.; Slibinskas, R.; Bechelanye, M.; Ramanavicius, A. Molecularly imprinted polypyrrole based sensor for the detection of SARS-CoV-2 spike glycoprotein. *Electrochim. Acta* **2022**, *403*, 139581. [[CrossRef](#)]
87. Li, T.; Wang, L.; Wang, H.; Li, X.; Zhang, S.; Xu, Y.; Wei, W. Serum SARS-CoV-2 Nucleocapsid Protein: A Sensitivity and Specificity Early Diagnostic Marker for SARS-CoV-2 Infection. *Front. Cell. Infect. Microbiol.* **2020**, *10*, 470. [[CrossRef](#)] [[PubMed](#)]
88. Nikolaev, E.N.; Indeykina, M.I.; Brzhozovskiy, A.G.; Bugrova, A.E.; Kononikhin, A.S.; Starodubtseva, N.L.; Petrotchenko, E.V.; Kovalev, G.I.; Borchers, C.H.; Sukhikh, G.T. Mass Spectrometric Identification of SARS-CoV-2 Proteins from Gargle Solution Samples of COVID-19 Patients. *J. Proteome Res.* **2020**, *19*, 4393–4397. [[CrossRef](#)] [[PubMed](#)]
89. Samper, I.C.; McMahan, C.J.; Schenkel, M.S.; Clark, K.M.; Khamcharoen, W.; Anderson, L.B.R.; Terry, J.S.; Gallichotte, E.N.; Ebel, G.D.; Geiss, B.J.; et al. Electrochemical Immunoassay for the Detection of SARS-CoV-2 Nucleocapsid Protein in Nasopharyngeal Samples. *Anal. Chem.* **2022**, *94*, 4712–4719. [[CrossRef](#)]
90. Białobrzaska, W.; Ficek, M.; Dec, B.; Osella, S.; Trzaskowski, B.; Jaramillo-Botero, A.; Pierpaoli, M.; Ryciewicz, M.; Dashkevich, Y.; Łęga, T.; et al. Performance of electrochemical immunoassays for clinical diagnostics of SARS-CoV-2 based on selective nucleocapsid N protein detection: Boron-doped diamond, gold and glassy carbon evaluation. *Biosens. Bioelectron.* **2022**, *209*, 114222. [[CrossRef](#)]
91. Karaman, C.; Yola, B.B.; Karaman, O.; Atar, N.; Polat, I.; Yola, M.L. Sensitive sandwich-type electrochemical SARS-CoV-2 nucleocapsid protein immunosensor. *Microchim. Acta* **2021**, *188*, 425. [[CrossRef](#)] [[PubMed](#)]
92. Eissa, S.; Alhadrami, H.A.; Al-Mozaini, M.; Hassan, A.M.; Zourob, M. Voltammetric-based immunosensor for the detection of SARS-CoV-2 nucleocapsid antigen. *Microchim. Acta* **2021**, *188*, 199. [[CrossRef](#)]
93. Aydın, E.B.; Aydın, M.; Sezgintürk, M.K. Label-free and reagent-less electrochemical detection of nucleocapsid protein of SARS-CoV-2: An ultrasensitive and disposable biosensor. *New J. Chem.* **2022**, *46*, 9172–9183. [[CrossRef](#)]
94. Wu, C.-C.; Chiang, Y.-H.; Chiang, H.-Y. A Label-Free Electrochemical Impedimetric Immunosensor with Biotinylated-Antibody for SARS-CoV-2 Nucleoprotein Detection in Saliva. *Biosensors* **2022**, *12*, 265. [[CrossRef](#)] [[PubMed](#)]
95. Li, J.; Lillehoj, P.B. Microfluidic Magneto Immunosensor for Rapid, High Sensitivity Measurements of SARS-CoV-2 Nucleocapsid Protein in Serum. *ACS Sens.* **2021**, *6*, 1270–1278. [[CrossRef](#)]
96. Tian, J.; Liang, Z.; Hu, O.; He, Q.; Sun, D.; Chen, Z. An electrochemical dual-aptamer biosensor based on metal-organic frameworks MIL-53 decorated with Au@Pt nanoparticles and enzymes for detection of COVID-19 nucleocapsid protein. *Electrochim. Acta* **2021**, *387*, 138553. [[CrossRef](#)]
97. Qi, H.; Hu, Z.; Yang, Z.; Zhang, J.; Wu, J.J.; Cheng, C.; Wang, C.; Zheng, L. Capacitive Aptasensor Coupled with Microfluidic Enrichment for Real-Time Detection of Trace SARS-CoV-2 Nucleocapsid Protein. *Anal. Chem.* **2022**, *94*, 2812–2819. [[CrossRef](#)] [[PubMed](#)]
98. Ramanathan, S.; Gopinath, S.C.B.; Ismail, Z.H.; Arshad, M.K.M.; Poopalan, P. Aptasensing nucleocapsid protein on nanodiamond assembled gold interdigitated electrodes for impedimetric SARS-CoV-2 infectious disease assessment. *Biosens. Bioelectron.* **2022**, *197*, 113735. [[CrossRef](#)] [[PubMed](#)]
99. Han, C.; Li, W.; Li, Q.; Xing, W.; Luo, H.; Ji, H.; Fang, X.; Luo, Z.; Zhang, L. CRISPR/Cas12a-Derived electrochemical aptasensor for ultrasensitive detection of COVID-19 nucleocapsid protein. *Biosens. Bioelectron.* **2022**, *200*, 113922. [[CrossRef](#)] [[PubMed](#)]
100. Raziq, A.; Kidakova, A.; Boroznjak, R.; Reut, J.; Öpik, A.; Syritski, V. Development of a portable MIP-based electrochemical sensor for detection of SARS-CoV-2 antigen. *Biosens. Bioelectron.* **2021**, *178*, 113029. [[CrossRef](#)]
101. Zhang, T.; Sun, L.; Zhang, Y. Highly sensitive electrochemical determination of the SARS-CoV-2 antigen based on a gold/graphene imprinted poly-arginine sensor. *Anal. Methods* **2021**, *13*, 5772–5776. [[CrossRef](#)]
102. Yousefi, H.; Mahmud, A.; Chang, D.; Das, J.; Gomis, S.; Chen, J.B.; Wang, H.; Been, T.; Yip, L.; Coomes, E.; et al. Detection of SARS-CoV-2 Viral Particles Using Direct, Reagent-Free Electrochemical Sensing. *J. Am. Chem. Soc.* **2021**, *143*, 1722–1727. [[CrossRef](#)]
103. Sukjee, W.; Thitithanyanont, A.; Manopwisedjaroen, S.; Seetaha, S.; Thepparit, C.; Sangma, C. Virus MIP-composites for SARS-CoV-2 detection in the aquatic environment. *Mater. Lett.* **2022**, *315*, 131973. [[CrossRef](#)]

104. Chaibun, T.; Puenpa, J.; Ngamdee, T.; Boonapatcharoen, N.; Athamanolap, P.; O'Mullane, A.P.; Vongpunsawad, S.; Poovorawan, Y.; Lee, S.Y.; Lertanantawong, B. Rapid electrochemical detection of coronavirus SARS-CoV-2. *Nat. Commun.* **2021**, *12*, 802. [[CrossRef](#)]
105. Kong, D.; Wang, X.; Gu, C.; Guo, M.; Wang, Y.; Ai, Z.; Zhang, S.; Chen, Y.; Liu, W.; Wu, Y.; et al. Direct SARS-CoV-2 Nucleic Acid Detection by Y-Shaped DNA Dual-Probe Transistor Assay. *J. Am. Chem. Soc.* **2021**, *143*, 17004–17014. [[CrossRef](#)]
106. Peng, Y.; Pan, Y.; Sun, Z.; Li, J.; Yi, Y.; Yang, J.; Li, G. An electrochemical biosensor for sensitive analysis of the SARS-CoV-2 RNA. *Biosens. Bioelectron.* **2021**, *186*, 113309. [[CrossRef](#)]
107. Hwang, C.; Park, N.; Kim, E.S.; Kim, M.; Kim, S.D.; Park, S.; Kim, N.Y.; Kim, J.H. Ultra-fast and recyclable DNA biosensor for point-of-care detection of SARS-CoV-2 (COVID-19). *Biosens. Bioelectron.* **2021**, *185*, 113177. [[CrossRef](#)] [[PubMed](#)]
108. Miripour, Z.S.; Sarrami-Forooshani, R.; Sanati, H.; Makarem, J.; Taheri, M.S.; Shojaeian, F.; Eskafi, A.H.; Abbasvandi, F.; Namdar, N.; Ghafari, H.; et al. Real-time diagnosis of reactive oxygen species (ROS) in fresh sputum by electrochemical tracing; correlation between COVID-19 and viral-induced ROS in lung/respiratory epithelium during this pandemic. *Biosens. Bioelectron.* **2020**, *165*, 112435. [[CrossRef](#)] [[PubMed](#)]
109. Samprathi, M.; Jayashree, M. Biomarkers in COVID-19: An Up-To-Date Review. *Front. Pediatr.* **2021**, *8*, 607647. [[CrossRef](#)] [[PubMed](#)]